Opdrachtgever:

Rijksinstituut voor Kust en Zee/RIKZ

Koppeling van GEMSED aan GEM

juli 2000

WL | delft hydraulics

Z2751

Koppeling van GEMSED aan GEM

E.J. Kranenborg
A.J. Nolte

juli 2000

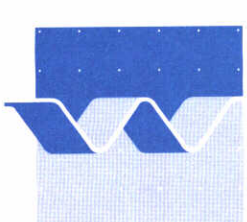

WL | delft hydraulics

WL | delft hydraulics

OPDRACHTGEVER:	DG Rijkswaterstaat Rijksinstituut voor Kust en Zee/RIKZ Tav. ir. M. Bokhorst Postbus 207 9750 AE Haren
TITEL:	Koppeling van GEMSED aan GEM

SAMENVATTING:

De module GEMSED berekent de flux van nutriënten (nitraat, ammonium en fosfaat) en zuurstof tussen de waterkolom en het sediment. De module is ontwikkeld door het Nederlands Instituut voor Onderzoek van de Zee (NIOZ) en toegepast als onderdeel van de ERSEM modellering van de Noordzee.

In het kader van het de operationalisering van het Generiek Ecologisch Model voor estuaria (GEM) is de module GEMSED beschikbaar gemaakt in (gekoppeld aan) het GEM instrumentarium. In dit rapport wordt een beschrijving geven van de functionaliteit van GEMSED, worden de gemaakte aannames ten behoeve van de koppeling beschreven en wordt de ontwikkelde koppeling getest door de gekoppelde GEMSED te vergelijken met een stand-alone versie van GEMSED.

Opdrachtgever is RIKZ, NIOZ is als onderaannemer voor de levering van GEMSED ingeschakeld.

REFERENTIES: Ruardij, van Raaphorst, 1995
Benthic nutrient regeneration in the ERSEM ecosystem model of the North Sea.
Neth. J Sea Research 33(3/4), pp 453-483.

VER.	AUTEUR		DATUM	OPMERK.	REVIEW		GOEDKEURING	
0.1	E. J. Kranenborg		15-06-2000		J.G.C. Smits		T. Schilperoort	
0.2	A.J. Nolte		05-07-2000		J.G.C. Smits		T. Schilperoort	
0.2a	A.J. Nolte	AN	24-07-2000	gecorrigeerd	A.N. Blauw	ANB	T. Schilperoort	
	E.J. Kranenborg							

PROJECTNUMMER:		Z2751						
TREFWOORDEN:		GEM, waterkwaliteit, bodemmodule, sediment-water uitwisseling						
INHOUD:	TEKST	14	TABELLEN	1	FIGUREN	2	APPENDICES	3
STATUS:	☐ VOORLOPIG		☐ CONCEPT		☒ DEFINITIEF			

Inhoud

Appendices

1 Inleiding

1.1 Achtergrond

In de afgelopen jaren is door WL | Delft Hydraulics in opdracht van RIKZ gewerkt aan de operationalisering van het Generiek Estuarium Model (GEM) op de Nederlandse kustzone (WL, 1999). GEM vormt een kader om tot integratie van Nederlandse kennis op het gebied van waterbeheer en waterkwaliteit te komen, middels integratie van de bij diverse instituten ontwikkelde en aan de praktijk getoetste deelmodellen. Het aldus ontstane instrument wordt gebruikt voor de kwantificering van de ecologische effecten als gevolg van de (voorgestelde) aanleg van infrastructurele werken in de Nederlandse kustzone en lozingsreductie.

GEM is afgeregeld op de kuststrook maar een nieuwe aanpak van nutrienten-nalevering uit de bodem is nodig, met name in de Waddenzee. Daartoe is besloten tot koppeling met de door het NIOZ ontwikkelde GEMSED bodemmodule. GEMSED is operationeel in het ERSEM-model (ontwikkeld door diverse Europese instituten) voor de ecologische modellering van de Noordzee. In GEMSED vindt een ten opzichte van DELWAQ meer geavanceerde modellering plaats van de fluxen van zuurstof, ammonium, nitraat, en fosfaat over het sediment-water grensvlak als gevolg van mineralisatie van organisch materiaal. Eerdere pogingen (vanaf 1997, zie (WL, 1997) en (WL, 1999)) om tot een werkende implementatie van de koppeling te komen waren gestrand op de afwezigheid van stand-alone testconfiguratie en een nog niet operationele set bibliotheek-routines voor GEMSED.

1.2 Doelstellingen

Onderhavig project had het volgende doel:

Koppeling van de module GEMSED aan het GEM instrumentarium, zodanig dat de module binnen GEM projecten ingezet kan worden.

Concreet betekent dit dat gewerkt is aan:

- Een werkende, standaard Fortran implementatie van de stand-alone GEMSED module volgens gedefinieerde specificaties (Ruardij, Raaphorst 1995), hetgeen is uitgevoerd door NIOZ als onderaannemer.
- Een werkende en geteste koppeling van de GEMSED module aan DELWAQ, te implementeren als een procesmodule uit de DELWAQ-processenbibliotheek.

Als resultaat van deze studie zijn de volgende producten opgeleverd:

- Onderhavig rapport waarin de voornaamste werkzaamheden en resultaten besproken worden;
- Een update van de GEM software met daarin geïmplementeerd de resultaten van het onderzoek.

1.3 Aanpak

De koppeling van GEMSED aan het GEM-instrumentarium is geïmplementeerd in de vorm van een nieuw Delwaq-procesmodule. Het implementatietraject wordt in hoofdstuk 3 beschreven.

1.4 Leeswijzer

Onderhavig rapport geeft een beschrijving van de implementatie-traject van de koppeling van de GEMSED-module aan het DELWAQ model. Het rapport is als volgt opgebouwd. In hoofdstuk 1 worden de achtergrond en de doelstellingen van het project beschreven.
Vervolgens wordt in hoofdstuk 2 de functionaliteit van de koppeling uitvoerig beschreven.
In hoofdstuk 3 wordt het implementatie-traject gepresenteerd. Tenslotte worden in hoofdstuk 4 aanbevelingen en conclusies gegeven. Appendix A bevat de formele omschrijving van de in- en uitvoer van de koppelingsmodule ten behoeve van praktisch gebruik in GEM-kader. Appendix B beschrijft de aanpak en resultaten van de testprocedure. Appendix C tenslotte bevat een uitvoerige, door het NIOZ geleverde functionele beschrijving van GEMSED.

1.5 Verantwoording

Het project is uitgevoerd onder leiding van F.J. Los door A.J. Nolte en E.J. Kranenborg in de periode van april 2000 tot en met juli 2000. In dezelfde periode werd P. Ruardij vanuit het NIOZ ingeschakeld voor de levering van de stand-alone GEMSED implementatie. De opdracht werd verleend in overeenkomst RKZ-817 dd. 13 april 2000.

2 Beschrijving GEMSED-DELWAQ koppeling

2.1 Functionaliteit en formuleringen

Een uitgebreide beschrijving van GEMSED wordt gegeven in Appendix C. Hier wordt volstaan met een kort overzicht.

GEMSED is een module die de concentratieprofielen van de nutriënten (NH_4, NO_3, PO_4) en zuurstof in het sediment berekent, en vervolgens de bijbehorende fluxen berekent op het grensvlak van de waterkolom en het sediment. De modellering van silicium is niet in de huidige module opgenomen.

Het onderliggende model (Ruardij, van Raaphorst, 1995, Appendix C is een bewerkte versie van dit artikel) is ontwikkeld voor de Noordzee en geïmplementeerd door het NIOZ. Bij de berekening van de profielen wordt rekening gehouden met diffusieprocessen en de invloed van redoxreacties in het sediment. De mineralisatie van organisch materiaal (de drijvende kracht achter de vorming van concentratiegradiënten) wordt niet expliciet binnen GEMSED uitgerekend maar wordt als invoer aan de module aangeboden. Mineralisatie en bioturbatie (i.e. aanpassing van de verticale distributie van gemineraliseerde componenten) worden geïmplementeerd in een schil rondom GEMSED, waarin de communicatie met het DELWAQ-gedeelte in GEM wordt voorzien.

In GEMSED worden de volgende stoffen gemodelleerd:
1. zuurstof;
2. nitraat;
3. ammonium;
4. fosfaat;
5. 'reductie-equivalenten'.

Bij de mineralisatie van organisch materiaal kan potentieel gebruik gemaakt worden van zuurstof (O_2), nitraat (NO_3^-), mangaan en ijzer (respectievelijk Mn(IV) en Fe(III)), sulfaat (SO_4^{2-}) en CO_2 als elektronen-acceptor. Het energetisch voordeel bij oxidatie van organisch koolstof is het grootst bij zuurstof en het laagst bij CO_2. Uiteindelijk kan vorming van methaan optreden. In GEMSED worden alle bovengenoemde acceptoren beschouwd. Echter, mangaan (II), ijzer (II), sulfide en methaan worden niet apart gemodelleerd, maar als 'reductie-equivalenten' samengenomen. Aangezien mangaan, ijzer en methaan van minder belang worden geacht in mariene milieus, worden aan de reductie-equivalenten de eigenschappen van sulfide (S^{2-}) toegekend (bijvoorbeeld de diffusiecoëfficiënt).

Op basis van de elektronen-acceptoren zijn in GEMSED drie lagen gedefinieerd:
1. aan het sediment-water grensvlak een oxische laag met zuurstof als elektronen-acceptor;
2. een denitrificatielaag met nitraat als elektronen-acceptor; en
3. een anoxische, sulfaat reducerende laag.

In ieder van de lagen wordt voor O_2, NO_3, NH_4, PO_4 en reductie-equivalenten het concentratieprofiel analytisch berekend. Daarbij worden de volgende processen en reacties in beschouwing worden genomen:

- mineralisatie van organisch materiaal waardoor ammonia, fosfaat en 'reductie-equivalenten' gevormd worden en zuurstof en nitraat verbruikt worden;
- nitrificatie;
- denitrificatie;
- adsorptie van ammonium en fosfaat;
- oxidatie van reductie-equivalenten;
- diffusief transport tussen de lagen;
- menging van de lagen door bioturbatie (in de DELWAQ-schil) en bio-irrigatie (binnen GEMSED).

De verticale posities van de grensvlakken - en daarmee de laagdiktes - zijn dynamische grootheden in GEMSED; zij hangen af van gemodelleerde variabelen. De dikte van de oxische laag wordt bepaald door de aanvoer van zuurstof door diffusie en de consumptie van zuurstof door mineralisatie, nitrificatie en oxidatie van 'reductie-equivalenten'. De dikte van de denitrificerende laag wordt bepaald door de snelheid van denitrificatie.

GEMSED werd ontwikkeld met als doel een snelle, doch zo nauwkeurig mogelijke evaluatie mogelijk te maken van de nutriëntfluxen over het sediment-water grensvlak, waarbij de analytische oplossing van de chemische evenwichten ondanks de beperkte gelaagdheid van het model, toch een hoge nauwkeurigheid oplevert. Het onderliggende conceptuele model wordt daarom analytisch opgelost, hetgeen alleen mogelijk is als de verschillende termen in de modelvergelijkingen een zeer eenvoudige formulering hebben:

- alle verliestermen zijn gemodelleerd als eerste-orde lineaire reacties, brontermen zijn gedefinieerd volgens nulde-orde kinetiek;
- adsorptie-processen zijn gedefinieerd als evenwichtsreacties;
- advectie van poriewater wordt als verwaarloosbaar transportproces beschouwd ten opzichte van diffusie; en
- diffusiecoëfficiënten en reactiesnelheden zijn onafhankelijk van de diepte.

2.2 Invoer GEMSED

GEMSED is aan het GEM-instrumentarium gekoppeld als een apart proces in de DELWAQ processenbibliotheek. Invoer voor GEMSED bestaat uit fluxen, concentraties, variabelen en constanten. De invoer voor GEMSED maakt gebruik van standaard DELWAQ functionaliteit, zoals de mogelijkheid op ruimtelijk- en/of tijdsafhankelijke variabelen op te geven.

In Figuur 2.1 worden de invoer en uitvoer van de GEMSED-module schematisch weergegeven. De module krijgt de benodigde invoer uit de overige GEM-modules en levert procesfluxen voor verschillende stoffen terug naar DELWAQ. Aangezien de mineralisatie van organisch materiaal in de bodem niet standaard binnen GEMSED wordt berekend, zijn de procesformuleringen uit de GEM-bodemmodule 'eenvoudige bodem' opgenomen in de GEMSED-module.

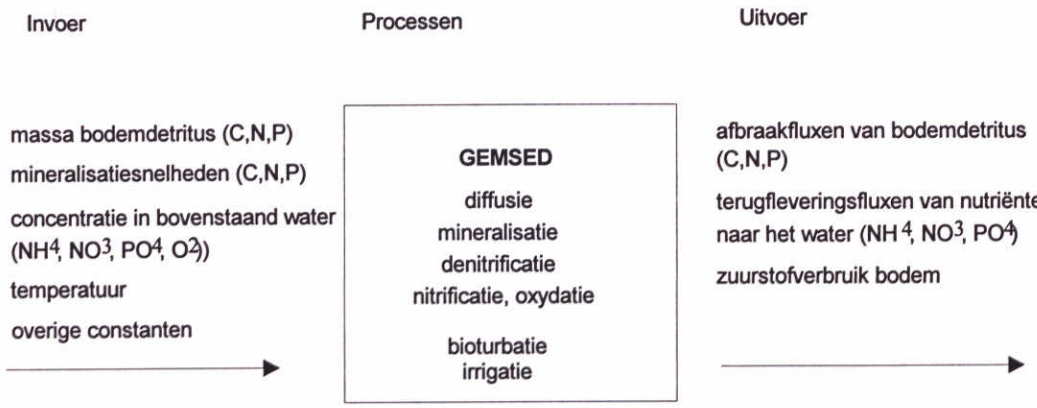

Figuur 2.1 Schematische weergave van de werking van GEMSED

Tabel 2.1 geeft een overzicht van alle variabelen en parameters die in GEMSED voorkomen. Indien aanwezig is de GEM variabele eveneens weergegeven (kolom 2). De overige termen in de tweede kolom zijn geclassificeerd zoals in het onderschrift van de tabel is weergegeven.
De eenheden die in de tabel vermeld worden, zijn de eenheden zoals vereist in GEMSED. Deze komen veelal niet overeen met de in GEM gebruikelijke eenheden. Uit oogpunt van consistentie wordt in GEM gebruik gemaakt van de gangbare eenheden. In de koppeling vindt vervolgens een conversie plaats van GEM eenheden naar GEMSED eenheden.

Tabel 2.1 Invoer variabelen GEMSED

Parameter in GEMSED	Parameter in GEM	omschrijving
concentratie waterkolom (mmol/m^3)		
O2o	OXY	zuurstofconcentratie in waterkolom
N4n	NH4	ammoniumconcentratie in waterkolom
N3n	NO3	nitraatconcentratie in waterkolom
N1p	PO4	fosfaatconcentratie in waterkolom
concentratie sediment (mmol/m^2)		
G2o	berekend	zuurstofconcentratie in oxische laag
K4n	berekend	ammoniumconcentratie in oxische laag
K14n	berekend	ammoniumconcentratie in denitrificatie + anoxische laag nitraatconcentratie in oxische + denitrificatie laag
K3n	berekend	fosfaatconcentratie in oxische + denitrificatie laag
K1p	berekend	fosfaatconcentratie in anoxische laag
K11p	berekend	concentratie reductie equivalenten in oxische + denitr. laag
K6e	berekend	concentratie reductie equivalenten in anoxische laag
K16e	berekend	
dikte sedimentlagen (m)		
D1m	berekend	dikte oxische laag
D2m	berekend	diepte van onderkant denitrificatie laag
Dtm	berekend	totaal dikte sediment

distributie van organisch materiaal in het sediment (m, '50%-diepte')		
D6m	invoer	diepteverdeling C in het sediment
D7m	invoer	diepteverdeling N in het sediment
D8m	invoer	diepteverdeling P in het sediment
Fluxen (mmol/m^3/d)		
rrBTo	invoer	C mineralisatie oxische laag
rrATo	invoer	C mineralisatie denitrificatie + anoxische laag
reBTn	invoer	N mineralisatie oxische laag
reATn	invoer	N mineralisatie denitrificatie + anoxische laag
reBTp	invoer	P mineralisatie oxische laag
reATp	invoer	P mineralisatie denitrificatie + anoxische laag
omgevingsvariabelen		
ETW	Temp	temperatuur (°C)
poro	poro	porositeit (-)
irrenh	invoer	bio-irrigatie (-)
reactiesnelheden bij 10 °C (1/d)		
sK4K3_p	invoer	nitrificatie
sK3G4_p	RcDenSed	denitrificatie
sOS_p	invoer	oxidatie van sulfide door zuurstof
rate (mmol/m^3/d)		
zATo_p	invoer	referentie anoxische mineralisatie snelheid waarop denitrificatie gelijk is aan sK3K4_p
concentratie (mmol/m^3)		
clM4n_p	invoer	kritische ammoniumconcentratie waaronder nitrificatie gelimiteerd is
clM6e_p	invoer	kritische red.eq. concentratie waaronder oxidatie van sulfide gelimiteerd is
limitatie (Michaelis-Menten)		
ehK3G4_p	invoer	maximaal toegestane vermenigvuldigingsfactor om denitrificatie te corrigeren voor anoxische mineralisatie (-)
adsorptie (-)		
pK1_ae	invoer	adsorptiecoëfficiënt fosfaat
pK11_p	invoer	adsorptiecoëfficiënt fosfaat anoxische laag
pK3_p	invoer	adsorptiecoëfficiënt nitraat
pK4_p	invoer	adsorptiecoëfficiënt ammonium
pK6_p	invoer	adsorptiecoëfficiënt anoxische equivalenten
Temperatuurafhankelijkheid voor diffusie (-)		
q10KI_p	invoer	temperatuurafhankelijkheid fosfaat
q10K3_p	invoer	temperatuurafhankelijkheid nitraat
q10K4_p	invoer	temperatuurafhankelijkheid ammonium
moleculaire diffusieconstanten bij 10 °C (m^2/d)		
xdiffG2	invoer	zuurstof
xdiffK1	invoer	fosfaat
xdiffK3	invoer	nitraat
xdiffK4	invoer	ammonium
xdiffK6	invoer	reductie equivalenten (gebaseerd op sulfide)

molverhouding reacties (-)		
qon_dentri_p	vaste waarde	O_2 : N in denitrificatie
qoK4n_p	vaste waarde	O_2 : N in nitrificatie
qro_p	vaste waarde	O_2 : S in sulfide oxidatie
parameters voor verandering laagdikte		
clD12m_p	invoer	minimale dikte denitrificatie laag (m)
clM3n_D2m_p	invoer	concentratie nitraat waaronder de anoxische laag begint
pmK3n_p	invoer	
chD1m_p	invoer	dikte van de oxische laag waarboven veranderingen worden gedempt (m)
xdampingDI_p	invoer	dempingsvariabele (-) voor verandering D1m, D2m
integratie in GEMSED		
rmax_p	invoer	maximaal toegestane verandering
mindelt_p	invoer	minimaal toegestane delta
massa → snelheid		
oneday_p	invoer	Niet geïmplementeerd, geen functie
opties (toekomstig)		
swWRITE_p	invoer	bewaar alle informatie voor profielen
overig		
depth / wdepth	Depth	waterdiepte (m)
dlt	Delt	tijdstap (d)

berekend: uitvoer van GEMSED (GEMSED-bodemvariabele);
invoer: invoerparameter, kan door de gebruiker gespecificeerd worden, anders wordt default waarde gebruikt;
vaste waarde: parameter met een vaste waarde, kan niet door gebruiker gewijzigd worden.

Uit tabel 2.1 valt af te leiden welke invoer door de gebruiker gespecificeerd moet worden. De invoer valt uiteen in een aantal groepen:

1. concentratie in de waterkolom → wordt gemodelleerd in GEM;
2. concentratie in het sediment → wordt berekend door GEMSED;
3. diverse constanten ten behoeve van reacties zoals nitrificatie snelheid → moeten door de gebruiker gespecificeerd worden;
4. diverse constanten ten behoeve van de analytische oplossing → zijn voor de gebruiker minder interessant omdat ze niet direct met de processen in het sediment te maken hebben. Er is echter voor gekozen om ze in ieder geval voor de gebruiker beschikbaar te maken;
5. omgevingsparameters → kunnen door GEM berekend worden (temperatuur), of kunnen door de gebruiker opgegeven worden (porositeit);
6. molverhoudingen → zijn vaste waarden en zijn niet voor de gebruiker beschikbaar gemaakt.

Uit tabel 2.1 komt een aantal invoerparameters naar voren die in de ERSEM-omgeving door andere modules worden aangeleverd maar in GEM niet aangeleverd kunnen worden. Zij corresponderen met de volgende processen of grootheden:

1. mineralisatiefluxen in de oxische dan wel denitrificatie + anoxische laag;
2. diepteverdeling van het organisch materiaal;
3. bioturbatie;

Genoemde processen en grootheden worden in de DELWAQ-schil geïmplementeerd zoals in secties 2.3 - 2.6 wordt beschreven. De bijbehorende parameters zijn in Appendix A beschreven.

2.3 Mineralisatieflux

De afbraak van organisch materiaal in ERSEM wordt door een andere module berekend en vervolgens aan GEMSED aangeleverd. Binnen GEM wordt de mineralisatie van organisch materiaal, dat door de toestandsvariabelen DetCS1, DetNS1 en DetPS1 weergegeven wordt, door het proces BOTMIN afgehandeld. De berekening van de mineralisatieflux gebruikt de volgende formulering:

$$dMin_i = \frac{ZMin_i}{Depth} + \frac{RC_i \times Tc_i^{(Temp-20)} \times i}{Volume}$$

waarin i = DetCS1, DetNS1 of DetPS1
$dMin_i$ = Mineralisatieflux ($g/m^3/d$)
$ZMin_i$ = nulde orde mineralisatieflux ($g/m^2/d$)
Depth = actuele diepte van het watersegment (m)
Rc_i = eerste orde mineralisatie snelheid (d^{-1})
Tc_i = temperatuur coëfficiënt voor mineralisatie (-)
Temp = water temperatuur
Volume = actueel volume van het watersegment (m^3)

De bovenstaande formulering is integraal in GEMSED overgenomen, zodat bijvoorbeeld de eerste orde mineralisatie snelheid bij de invoer van GEMSED moet worden opgegeven.

De op deze wijze berekende mineralisatieflux is de totale mineralisatieflux in het gehele sediment, terwijl in GEMSED als invoer de mineralisatieflux in de oxische laag en de denitrificatie laag + anoxische laag gespecificeerd moet worden. Om de berekende totale mineralisatieflux op te splitsen naar de lagen, wordt gebruikt gemaakt van de verdeling van het organisch materiaal, zoals hiernavolgend beschreven.

De verdeling van het organisch materiaal in de bodem volgt een exponentieel verloop welke gegeven wordt door de onderstaande formule:

$$I = \frac{(e^{\alpha \times d} - 1)}{\alpha}$$

waarin I = gewichtsfunctie
α = constante voor diepte verdeling organisch materiaal (m^{-1})
d = diepte vanaf het sediment-water grensvlak (m)

De vorm van de gewichtsfunctie wordt weergegeven in figuur 2.2a. De functie moet geïnterpreteerd worden als een gewichtsfunctie die aangeeft wat de fractie van het organisch materiaal is dat zich boven een bepaalde diepte bevindt. Aan het sediment-water

grensvlak is de fractie 0, op maximale diepte van het sediment is de fractie 100%. Dit is weergegeven in figuur 2.2b.

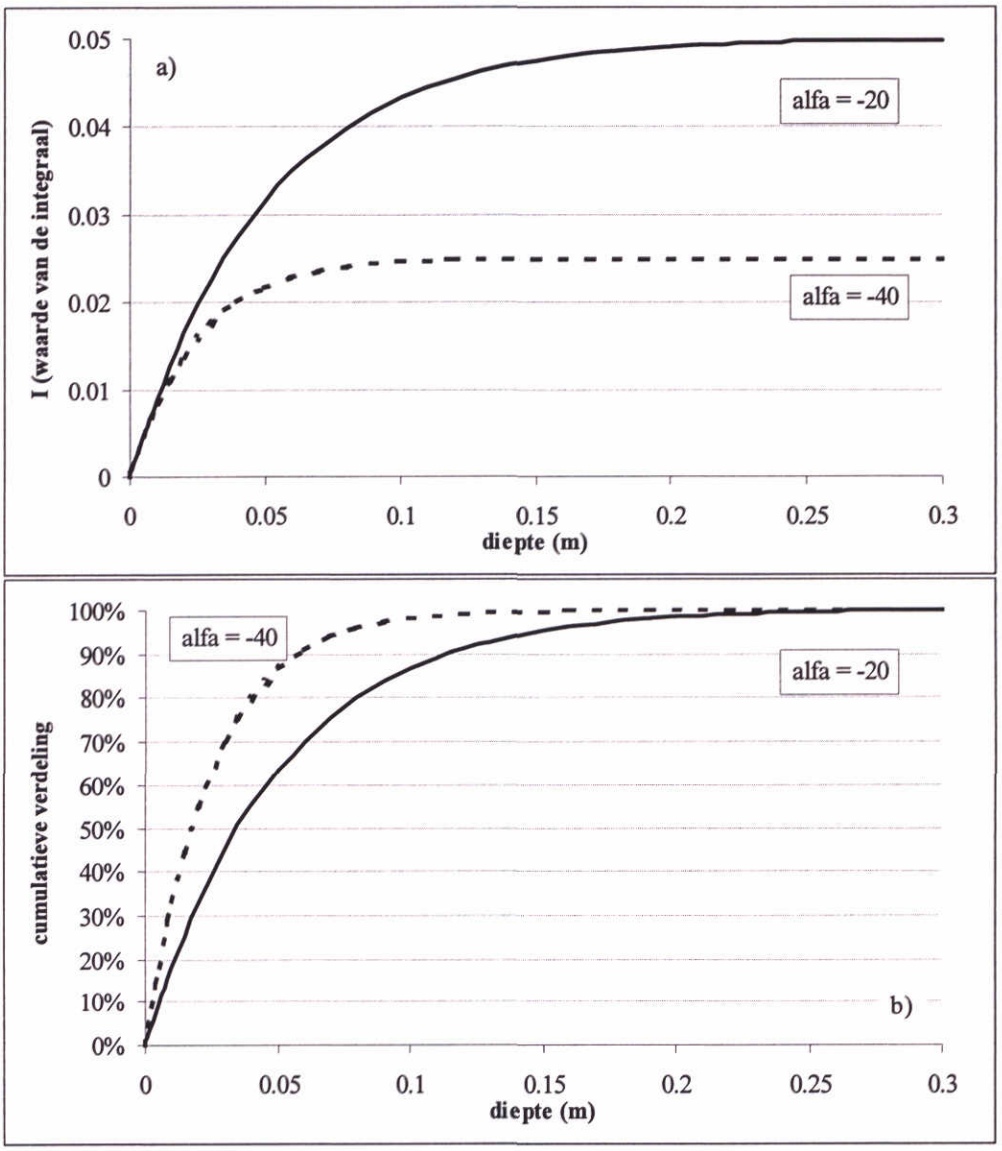

Figuur 2.2 a) Verdeling van organisch materiaal over de diepte met alfa = -20 m^{-1} en alfa = -40 m^{-1} volgens de integraal en b) percentuele verdeling organisch materiaal over de diepte met alfa = -20 m^{-1} en alfa = -40 m^{-1}.

De waarde van α is derhalve bepalend voor de verdeling van organisch materiaal in het sediment (de maximale diepte van het sediment is in dit voorbeeld 0,30 m gekozen). Uit figuur 2.2a blijkt dat de waarde van de functie naar $-1/\alpha$ loopt als de diepte groot genoeg wordt. Verder blijkt uit figuur 2.2b dat de fractie van het organisch materiaal in het bovenste gedeelte groter wordt naarmate de waarde van alfa groter is.

De totale mineralisatieflux wordt nu opgesplitst op basis van de fractionele verdeling van het organisch materiaal:

$$dMin_{i\_ox} = dMin_i \times \frac{f(\alpha, z_{ox})}{f(\alpha, z_{tot})} \times Factor$$

$$dMin_{i\_anox} = dMin_i - dMin_{i\_ox}$$

waarbij $dMin_{i\_ox}$ = mineralisatieflux in de oxische laag
$dMin_{i\_anox}$ = mineralisatieflux in de denitrificatie laag + de anoxische laag
$f(\alpha, z)$ = waarde van de integraal met waarde van α en dikte van de oxische laag (z_{ox}) en de totale laagdikte van het sediment (Z_{tot})
Factor = vermenigvuldigingsfactor voor de mineralisatieflux in de oxische laag

De vermenigvuldigingsfactor is aan de formulering toegevoegd om af te kunnen wijken van de standaard verdeling van het organisch materiaal. De gedachte erachter is dat het organisch materiaal in de oxische laag verser is en sneller afgebroken kan worden. Door de Factor gelijk aan bijvoorbeeld 1,1 te zetten, neemt de mineralisatieflux in de oxische laag met 10% toe ten opzichte van de 'standaard' verdeling van het organisch materiaal. Dit gaat ten koste van mineralisatie in de overige lagen, omdat de totale mineralisatie gelijk blijft.

2.4 Geadsorbeerd fosfaat

In GEMSED komt geadsorbeerd fosfaat niet als toestandvariabele voor. De totale pool wordt gemodelleerd en de concentratie fosfaat in het poriewater wordt bepaald aan de hand van een distributiecoëfficiënt:

$$PO4_{totaal} = PO4_{opgelost} + PO4_{geadsorbeerd} = PO4_{opgelost} \times (1 + K_D)$$

In GEM daarentegen wordt geadsorbeerd fosfaat actief als toestandsvariabele gemodelleerd (AAP in de waterkolom, AAPS1 in het sediment), terwijl de fosfaatconcentratie in het poriewater niet bekend is. In de invoer van GEMSED moet derhalve de geadsorbeerde pool bij de totale fosfaat pool gerekend worden.

Voor de verdeling van AAPS1 in het sediment wordt op pragmatische gronden dezelfde verdeling (α) als voor organisch P aangenomen. Met gebruikmaking van de distributie-coëfficiënt (K_D) wordt de nieuwe initiële conditie voor de totale fosfaatconcentratie in de sedimentlagen bepaald:

$$PO4_{opgelost} = \frac{PO4_{totaal}}{(1 + K_D)}$$

$$PO4_{geadsorbeerd} = AAPS1 \times \frac{f(\alpha, z_{den})}{f(\alpha, z_{tot})}$$

$$PO4_{totaal} = PO4_{opgelost} + PO4_{geadsorbeerd}$$

waarbij z_{den} = de diepte van de denitrificatie laag

Eenzelfde set vergelijkingen geldt voor de anoxische laag. Vervolgens wordt door GEMSED de nieuwe totaal fosfaatconcentratie per laag berekend, waaruit met behulp van de distributiecoëfficiënt de nieuwe AAPS1 per laag berekend wordt.

2.5 Bio-irrigatie

Bio-irrigatie is de menging van het poriewater in het sediment door organismen. Door opname en uitscheiding van poriewater treedt een verplaatsing van het poriewater. In ERSEM wordt de bio-irrigatie bepaald door de organismen te modelleren. Bio-irrigatie is vervolgens geïmplementeerd als een vermenigvuldiging van de diffusiecoëfficiënt volgens,

$$D = (1+irr)D_m,$$

waarbij D = diffusiecoëfficiënt gecorrigeerd voor irrigatie
irr = irrigatiecoëfficiënt
D_m = moleculaire diffusiecoëfficiënt

Aangezien in GEM geen bodemorganismen gemodelleerd worden, is ervoor gekozen bio-irrigatie slechts als een constante (*irr*) in de invoer van GEMSED op te nemen.

2.6 Bioturbatie

Door de activiteit van organismen in het sediment verandert de verdeling van het organisch materiaal. In ERSEM wordt bioturbatie berekend door de organismen zelf te modelleren, en wordt respiratie van bodemorganismen gerelateerd aan bioturbatie.

In GEMSED wordt de diepteverdeling van het organisch materiaal aangepast volgens (*D6m* voor C, *D7m* voor N, *D8m* voor P):

$$D6m^{\text{nieuw}} = D6m + 2\times10^{-6} \times Factor \times (1 - e^{(-0,02/D6m)}) / D6m$$

waarbij D6m = Diepte parameter (=1/α) (-)
2×10^{-6} = diffusie gerelateerde parameter (-)
Factor = vermenigvuldigingsfactor voor de diffusie (-)

Binnen ERSEM wordt de *Factor* aangeleverd door andere modules. Overigens heeft de *Factor* in ERSEM een bovengrens van 10. Binnen GEMSED moet de waarde door de gebruiker opgegeven worden.

3 Implementatie-traject

De implementatie van GEMSED-DELWAQ koppeling heeft plaatsgevonden in vier fasen:

a) Formele definitie van de koppeling (uitgebreid t.o.v. eerdere GEM-rapportage (WL 1999));
b) Door het ontbreken van mineralisatie- en bioturbatie-modellering in GEMSED zijn deze processen in de koppelingsschil geïmplementeerd. Het effect van deze processen dient bij operationeel gebruik getest te worden;
c) Operationeel maken van GEMSED in een stand-alone omgeving (door NIOZ, zie Appendix C);
d) Operationeel maken van Stand-alone GEMSED op voor Delft3D relevante computer-platforms (Diverse UNIX-platforms, WIN95, NT);
e) Ontwikkeling en test van de GEMSED-DELWAQ koppeling op voor Delft3D relevante computer-platforms.

Ad c: GEMSED stand-alone:
GEMSED is voorheen alleen gebruikt als onderdeel van het ERSEM-model. Voor de toepassing in het GEM-instrumentarium is GEMSED geschikt gemaakt om als zelfstandige module te rekenen, met invoer van en uitvoer naar het GEMSED-instrumentarium. Met de stand-alone versie van GEMSED (i.e. zonder koppelingsschil) zijn de volgende tests uitgevoerd:

- Bereiken van een evenwichtsoplossing bij afwezigheid van chemische reacties. Doel van deze test is een controle van de transportmodellering binnen de stand-alone GEMSED module. De oplossingen zijn vergeleken met analytische oplossingen van de modelvergelijkingen.
- Bereiken van een evenwichtsoplossing bij opgave van constante brontermen. Doel van deze test is de controle van reactie-modellering binnen de stand-alone GEMSED module. De oplossingen zijn vergeleken met analytische oplossingen van de modelvergelijkingen. Deze test is de meest uitgebreide test die vergelijkingen met analytische oplossingen mogelijk maakt.

Ad d: Koppeling GEMSED-DELWAQ:
Als interface tussen GEM en GEMSED is een koppelingsmodule geschreven. Deze module is onderdeel van de GEMSED-module en vormt als het ware de stekker naar de rest van het GEM-instrumentarium. De formele beschrijving van de in- en uitvoer van de koppeling is in appendix A gegeven. Deze beschrijving dient als hulp bij de operationalisatie van de koppeling in concrete waterkwaliteitsproblemen.

Om het functioneren van de module te beoordelen is zij getest, zodanig dat een directe vergelijking met de resultaten van de stand-alone GEMSED-module mogelijk is. Daartoe zijn bij toepassing van de stand-alone module mineralisatie en bioturbatie als forcing functions voorgeschreven. Getest is op een DELWAQ model met één segment. De beschrijving van deze test en de test-resultaten is in appendix B weergegeven.

4 Conclusies en aanbevelingen

Op grond van het positieve testresultaat kan geconcludeerd worden dat een koppeling van GEMSED aan DELWAQ geslaagd is, met behoud van volledige functionaliteit (alle voor de gebruiker relevante parameters beschikbaar voor specificatie) en integriteit (geen wijziging van de GEMSED-code, GEMSED functioneert in de koppeling consistent met de stand-alone versie) van de GEMSED-module. Aangezien het uitvoeren van een test met een operationeel model niet tot de doelstellingen van dit project hoort, kunnen op dit moment geen conclusies over het praktisch functioneren van de koppeling getrokken worden.

Voor de toepassing van de koppelingsmodule in de GEM-praktijk hebben wij de volgende aanbevelingen:

a) Door het ontbreken van mineralisatie- en bioturbatie-modellering in GEMSED zijn deze processen in de koppelingsschil geïmplementeerd. Het effect van deze processen dient bij operationeel gebruik getest te worden.
b) Er bestaan aanzienlijke conceptuele verschillen tussen DELWAQ en GEMSED: zo zijn negatieve zuurstof-concentraties in DELWAQ wel maar in GEMSED niet mogelijk. Bovendien mogen in GEMSED bodemlagen niet verdwijnen en zijn limiet-condities als nul-concentraties en afwezige mineralisatie-fluxen niet toegestaan. Hoewel deze limiet-condities in de koppeling zijn afgevangen door het garanderen van zeer kleine concentraties en fluxen, moet bij de analyse van modelresultaten rekening gehouden te worden met het effect van deze condities.
c) Door het ontbreken van praktische ervaring met de koppeling is de performance van de koppelingsmodule in verhouding tot DELWAQ nog niet bekend. Het is daarom raadzaam een aantal performance-testen uit te voeren gebaseerd op tijdstapgrootte. In het geval de koppelingsmodule de vertragende factor blijkt, is aggregatie van segmenten een optie.

5 Literatuur

Ruardij, van Raaphorst, 1995
Benthic nutrient regeneration in the ERSEM ecosystem model of the North Sea. Neth. J Sea Research 33(3/4), pp 453-483.

WL, 1997
GEM, a Generic Ecological Model for estuaries. Model documentation T2087. WL | Delft Hydraulics (J.G.C. Smits, M. Bokhorst, A.G. Brinkman, P.M.J. Herman, P. Ruardij, H.L.A. Sonneveldt en M.W.M. van der Tol)

WL, 1999
Toepassing van GEM op de Nederlands Kustwateren. Rapport Z2556. WL | Delft Hydraulics (A.N. Blauw, F.J. Los, E.J. Kranenborg, J.G. Boon)

A Beschrijving I/O Koppeling

In DELWAQ is de GEM-GEMSED-koppeling als procesmodule geïmplementeerd. In deze appendix wordt de formele specificatie van de input en output van deze module gegeven, ter referentie bij het implementeren van operationele modellen waarin deze procesmodule toegepast wordt.

De met de GEM-GEMSED-koppeling corresponderende parameterlijst bestaat uit een viertal blokken die opgebouwd zijn uit de volgende parameters:

- Invoergrootheden op segment-niveau
- Uitvoergrootheden op segment-niveau
- Fluxen op segment-niveau
- Stoichiometrie

De eenheden worden geintroduceerd en parameters worden waar nodig toegelicht. Alle parameters zijn met hun DELWAQ naam weergegeven.

Invoergrootheden op segment-niveau:

De parameters in dit invoerblok worden bij iedere aanroep van de koppelingsmodule door DELWAQ als invoer-parameters aangeboden. Vrijwel alle parameters uit tabel 3.1 komen in dit blok voor, aangezien het uitgangspunt is geweest alle relevante interne GEMSED-parameters aan de gebruiker beschikbaar te stellen. Additionele parameters hebben betrekking op begincondities voor het onderliggende GEMSED-model (parameters met de namen init***) en de in de koppeling geïmplementeerde mineralisatie- en transport-processen (irrigatie, bioturbatie). Als laatste zijn de toestandsvariabelen van GEMSED toegevoegd (zie beschrijving eenheid uitvoergrootheden). Opgemerkt dient te worden dat bodemvariabelen gedefinieerd zijn in termen van volume-eenheid (of oppervlakte-eenheid) sediment, met uitzondering van de beginvoorwaarden init***, welke in termen van poriewater-concentratie zijn weergegeven om specificatie in termen van waterkolom-concentraties mogelijk te maken.

Weergave invoer-blok in parameterlijst:

GEMSED	GEM nutrient sediment model	
GEMSED	; naam module	
123	; waarde van TRswitch	
83	; aantal invoer grootheden op segment niveau	
OXY	Oxygen concentration in water column	(g/m3)
NH4	Ammonium concentration in water column	(gN/m3)
NO3	Nitrate concentration in water column	(gN/m3)
PO4	Phosphate concentration in water column	(gP/m3)
initOXYS1	Oxygen concentration in oxic layer	(g/m3)
initNH4S1	Ammonium concentration in oxic layer	(gN/m3)
initNH4S2	Ammonium concentration in anoxic layer	(gN/m3)
initNO3S1	Nitrate concentration in oxic layer	(gN/m3)
initPO4S1	Phosphate concentration in oxic layer	(gP/m3)

initPO4S2	Phosphate concentration in anoxic layer	(gP/m3)
initREDS1	Reduced equivalents in oxic layer	(g/m3)
initREDS2	Reduced equivalents in anoxic layer	(g/m3)
initD1M	Thickness oxic layer	(m)
initD2M	Depth upperside anoxic layer	(m)
initDTM	Total sediment thickness	(m)
initDistrC	Depth distribution of detritus C fraction	(m)
initDistrN	Depth distribution of detritus N fraction	(m)
initDistrP	Depth distribution of detritus P fraction	(m)
ZMinDetCS1	zeroth-order C-min. flux sediment S1	(gC/m2/d)
DetCS1	mass carbon detritus sediment S1	(gC)
RcDetCS1	first-order C-min. rate const. sediment S1	(1/d)
TcBMDetC	temp. coefficient C-min. in sediment	(-)
ZMinDetNS1	zeroth-order N-min. flux sediment S1	(gN/m2/d)
DetNS1	mass nitrogen detritus sediment S1	(gN)
RcDetNS1	first-order N-min. rate const. sediment S1	(1/d)
TcBMDetN	temp. coefficient N-min. in sediment	(-)
ZMinDetPS1	zeroth-order P-min. flux sediment S1	(gP/m2/d)
DetPS1	mass phosphorus detritus sediment S1	(gP)
RcDetPS1	first-order P-min. rate const. sediment S1	(1/d)
TcBMDetP	temp. coefficient P-min. in sediment	(-)
AAPS1	mass adsorbed phosphates sediment S1	(gP)
Factor_min	scaling factor for detritus distr. in sediment	(-)
Factor_trb	scaling factor for detritus distr. in sediment	(-)
TEMP	Ambient water temperature	(oC)
CTMin	critical temperature for mineralisation	(oC)
poros	porosity	(-)
bio_irr	Bio-irrigation factor	(-)
RcNitSed	Nitrification rate oxic layer at 10 oC	(1/d)
RcDenSed	Denitrification rate in sediment at 10 oC	(1/d)
RcReoxSed	Reoxidation rate in the sediment at 10 oC	(1/d)
KdPO4S1	Adsorption coefficient PO4 oxic layer	(-)
KdPO4S2	Adsorption coefficient PO4 anoxic layer	(-)
KdNO3	Adsorption coefficient NO3 in the sediment	(-)
KdNH4	Adsorption coefficient NH4 in the sediment	(-)
KdRED	Adsorption coeff. Reduced equiv. in sediment	(-)
DiffOXY	Oxygen diffusion constant at 10 oC	(m2/d)
DiffPO4	Phosphate diffusion constant at 10 oC	(m2/d)
DiffNO3	Nitrate diffusion constant at 10 oC	(m2/d)
DiffNH4	Ammonium diffusion constant at 10 oC	(m2/d)
DiffRED	Reduced equiv. diffusion constant at 10 oC	(m2/d)
TcDiffPO4	Temperature dependence PO4 diffusion	(-)
TcDiffNO3	Temperature dependence NO3 diffusion	(-)
TcDiffNH4	Temperature dependence NH4 diffusion	(-)
Depth	Depth of DELWAQ segment	(m)
Volume	volume calculated by DELWAQ	(m3)
zATo_p	Reference rate of anoxic mineralisation	(g/m2/d)
clM4n_p	Low concentr. nitrification limitation	(g/m2)
clM6e_p	Low concentr. reoxidation limitation	(g/m2)
MinThDen	Minimal thickness denitrification layer	(m)
MinNO3	NO3 conc. below which anoxic layer begins	(g/m2)
ehK3G4_p	Max. correction factor for anoxic miner.	(-)
pmK3n_p	NO3 fraction at and of denitrification layer	(-)
chD1m_p	Thickness oxic layer for damping	(m)
xdamping	Power to damp changes in layer thickness	(-)
rmax_p	Maximum allowed change	(-)
mindelt_p	Minimum allowed time step	(d)
oneday_p	mass - rate conversion	(-)
Delt	DELWAQ Time step for a single integration	(d)
SURF	Surface area of segment	(m2)
OXYS1	Oxygen concentration in oxic layer	(g/m2)
NH4S1	Ammonium concentration in oxic layer	(gN/m2)
NH4S2	Ammonium concentration in anoxic layer	(gN/m2)
NO3S1	Nitrate concentration in oxic layer	(gN/m2)

PO4S1	Phosphate concentration in oxic layer	(gP/m2)
PO4S2	Phosphate concentration in anoxic layer	(gP/m2)
REDS1	Reduced equivalents in oxic layer	(g/m2)
REDS2	Reduced equivalents in anoxic layer	(g/m2)
D1M	Thickness oxic layer	(m)
D2M	Depth upperside anoxic layer	(m)
DTM	Total sediment thickness	(m)
DistrC	Depth distribution of detritus C fraction	(m)
DistrN	Depth distribution of detritus N fraction	(m)
DistrP	Depth distribution of detritus P fraction	(m)

0 ; aantal invoer items op exchange niveau

Uitvoergrootheden op segment-niveau:

In dit blok zijn de interne GEMSED-variabelen opgenomen. Deze parameters dienen door de gebruiker onaangetast gelaten te worden aangezien ze gebruikt worden om de interne status van GEMSED voor een volgende tijdstap veilig te stellen (voor elke tijdstap wordt de koppelingsmodule aangeroepen en weer verlaten, waardoor het beheer van de interne GEMSED-toestandsvariabelen bij de koppelingsmodule komt te liggen).

Weergave uitvoer-blok in parameterlijst:

14 ; aantal uitvoer grootheden op segment niveau

OXYS1	Oxygen concentration in oxic layer	(g/m2)
NH4S1	Ammonium concentration in oxic layer	(gN/m2)
NH4S2	Ammonium concentration in anoxic layer	(gN/m2)
NO3S1	Nitrate concentration in oxic layer	(gN/m2)
PO4S1	Phosphate concentration in oxic layer	(gP/m2)
PO4S2	Phosphate concentration in anoxic layer	(gP/m2)
REDS1	Reduced equivalents in oxic layer	(g/m2)
REDS2	Reduced equivalents in anoxic layer	(g/m2)
D1M	Thickness oxic layer	(m)
D2M	Depth upperside anoxic layer	(m)
DTM	Total sediment thickness	(m)
DistrC	Depth distribution of detritus C fraction	(m)
DistrN	Depth distribution of detritus N fraction	(m)
DistrP	Depth distribution of detritus P fraction	(m)

0 ; aantal uitvoer items op exchange niveau

Fluxen op segment-niveau:

In dit blok wordt de uitvoer van de koppelingsmodule beschreven. Deze uitvoer bestaat uit de door GEMSED geleverde bodem-waterfluxen (dGEMSED***) alsmede de in de koppeling berekende mineralisatie-fluxen (dMINER***) en de fosfaat-adsorptieflux (dAAPS1). De parameters uit dit blok worden via de in het volgende blok gedefinieerde stoichiometrie gekoppeld aan de DELWAQ-variabelen.

Weergave fluxen in parameterlijst:

```
 8     ; aantal fluxen (sediment --> water is positive flux)
dGEMSEDOXY          Sediment oxygen demand GEMSED          (g/m3/d)
dGEMSEDNH4          Sediment-water flux NH4                (gN/m3/d)
dGEMSEDNO3          Sediment-water flux NO3                (gN/m3/d)
dGEMSEDPO4          Sediment-water flux                    (gP/m3/d)
dMINERCO2           miner. src. DetCS1 to GEMSED (C02)     (gC/m3/d)
dMINERNH4           miner. src. DetNS1 to GEMSED (NH4)     (gN/m3/d)
dMINERPO4           miner. src. DetPS1 to GEMSED (PO4)     (gP/m3/d)
dAAPS1              adsorbtion difference                  (gP/m3/d)
```

Stoichiometrie:

In dit blok wordt beschreven hoe de DELWAQ-variabelen in het onderste segment van de waterkolom en de detritus-fracties (Det*S1) worden gekoppeld aan de berekende fluxen uit de voorgaande module. In de eerste kolomn staan de DELWAQ-variabelen, in de tweede kolom de fluxen, en in de derde kolom de stoichiometrische schalingsfactoren.

Weergave stoichiometrie in procesmodule:

```
 11    ; aantal basis stochiometrie termen
OXY             dGEMSEDOXY          1.0     ;Net oxygen demand due to Corg
                                            mineralisation and nitrification
NH4             dGEMSEDNH4          1.0
NO3             dGEMSEDNO3          1.0
PO4             dGEMSEDPO4          1.0
CO2             dMINERCO2           1.000   ;CO2(aq) in sediment released
                                            immediately to DELWAQ seg.
H+              dMINERNH4           -0.071  ;H+ in sediment released immediately to
                                            DELWAQ seg.
H+              dMINERPO4           0.097   ; „  „   „   „   „
DetCS1          dMINERCO2           -1.000  ;(H+ is not modelled by GEMSED)
DetNS1          dMINERNH4           -1.000
DetPS1          dMINERPO4           -1.000
AAPS1           dAAPS1              -1.000
 0     ; aantal basis stochiometrie termen velocity-arrays
 0     ; aantal basis stochiometrie termen dispersie-arrays
END
```

B Test Koppeling

In deze appendix staan de testopzet en de testresultaten voor de koppelingsmodule beschreven. Doel van de test is te verifiëren dat de GEM-koppeling en de stand-alone GEMSED implementaties dezelfde resultaten geven voor een overeenkomstige invoer, en daarmee aan te tonen dat GEMSED in de koppelingsmodule functioneert en de informatie-overdracht in de koppeling via parameters en variabelen correct verloopt.

Test-opzet

De GEM-koppeling en stand-alone GEMSED module moeten onder vergelijkbare condities dezelfde resultaten leveren.
Allereerst is een scenario voor de GEM-koppeling gedefinieerd. Er is uitgegaan van een model met een DELWAQ-segment, waarbij de concentraties van zuurstof, ammoniak, nitraat en fosfaat in de waterkolom (constant in de tijd) als randvoorwaarde voor de bodem-module zijn voorgeschreven. Tevens zijn beginvoorwaarden voor de toestandsvariabelen van de bodemmodule gedefinieerd. Resultaten (i.e. de toestandvariabelen van de bodem-module) zijn bij aanvang van de simulatie en na een tijdstap opgeslagen ter vergelijking met de resultaten van de stand-alone GEMSED module. Bovendien is de overdracht van alle parameters uit DELWAQ (corresponderend met het overzicht in Appendix A) gecontroleerd op correctheid (met name conversie van massa- en volume-eenheden).
Vervolgens zijn de resultaten van de stand-alone GEMSED module gegenereerd door een eenmalige aanroep van GEMSED waarbij de variabelen, mineralisatie-fluxen en parameters dezelfde waarden hebben als de waarden bij uitvoering van de test van de koppelings-procedure precies bij aanroep van de bodemmodule.

Test-resultaten

Gebaseerd op de volgende beginvoorwaarden en parameters (overgenomen uit DELWAQ invoer-file)

```
; constant values
8     ;'initOXYS1'
5e-2  ;'initNH4S1'
5e-2  ;'initNH4S2'
1e-1  ;'initNO3S1'
1e-2  ;'initPO4S1'
1e-2  ;'initPO4S2'
1e-2  ;'initREDS1'
1e-2  ;'initREDS2'
0.01  ;'initD1M'
0.05  ;'initD2M'
0.30  ;'initDTM'
0.05  ;'initDistrC'
0.05  ;'initDistrN'
0.05  ;'initDistrP'
0.0   ;'ZMinDetCS1'
1e3   ;'DetCS1'
3e-2  ;'RcDetCS1'
1.09  ;'TcBMDetC'
0.0   ;'ZMinDetNS1'
1e3   ;'DetNS1'
3e-2  ;'RcDetNS1'
1.09  ;'TcBMDetN'
0.0   ;'ZMinDetPS1'
1e3   ;'DetPS1'
3e-2  ;'RcDetPS1'
1.09  ;'TcBMDetP'
0.0   ;'AAPS1'
```

```
1.0   ;'Factor_min'
10.0  ;'Factor_trb'
15    ;'TEMP'
3.0   ;'CTMin'
0.4   ;'poros'
5     ;'bio_irr'
1.5   ;'RcNitSed'
0.42  ;'RcDenSed'
0.25  ;'RcReoxSed'
250   ;'KdPO4S1'
2     ;'KdPO4S2'
0     ;'KdNO3'
3.0   ;'KdNH4'
0     ;'KdRED'
4.5E-4 ;'DiffOXY'
64.8E-6;'DiffPO4'
164.E-6;'DiffNO3'
173.E-6;'DiffNH4'
60.E-6 ;'DiffRED'
1.419  ;'TcDiffPO4'
2.0    ;'TcDiffNO3'
2.0    ;'TcDiffNH4'
0.448  ;'zATo_p'
0.0014 ;'clM4n_p'
3.206  ;'clM6e_p'
0.01   ;'MinThDen'
0.007  ;'MinNO3'
30.0   ;'ehK3G4_p'
0.1    ;'pmK3n_p'
0.05   ;'chD1m_p'
2.0    ;'xdamping'
0.2    ;'rmax_p'
1E-8   ;'mindelt_p'
1.0    ;'oneday_p'
 1.00000e+00 ; ACTIVE_GEMSED
 0.00000e+000 ; ACTIVE_VERTDISP
 1.00000e+000 ; ACTIVE_TOTDEPTH
 1.00000e+000 ; ACTIVE_DYNDEPTH
 1.00000e+000 ; CLOSE_ERR
 1.00000e+002 ; MaxIter
 1.00000e-007 ; Tolerance
 0.00000e+000 ; Iteration Report
 1.00000e+000 ; ONLY_ACTIVE
```

zijn de volgende resultaten gegenereerd (massa-eenheden zijn weergegeven in mmol i.p.v. gram ten behoeve van vergelijking met stand-alone GEMSED):

Naam bodem-variabele	waarde voor aanroep bodemmodule	waarde na aanroep bodemmodule koppeling	waarde na aanroep standalone GEMSED
OXYS1	1.0	0.97513	0.97513
NH4S1	$5.71428\ 10^{-2}$	5.69680 10-2	5.69680 10-2
NH4S2	1.65714	1.66189	1.66189
NO3S1	0.85714	0.81716	0.81716
PO4S1	$6.45161\ 10^{-3}$	1.23606 10-2	1.23606 10-2
PO4S2	$3.22581\ 10^{-2}$	3.02139 10-2	3.02139 10-2
REDS1	$1.24766\ 10^{-3}$	1.55711 10-3	1.55711 10-3
REDS2	$3.61822\ 10^{-2}$	3.57110 10-2	3.57110 10-2
D1m	$1\ 10^{-2}$	1 10-2	1 10-2
D2m	$5\ 10^{-2}$	5.00140 10-2	5.00140 10-2

De resultaten na een tijdstap zijn voor zowel de koppeling als de stand-alone module identiek. Hiermee is aangetoond dat GEMSED in de koppeling op identieke wijze als de stand-alone versie opereert. Tevens is aangetoond dat de parameter-overdracht vanuit DELWAQ naar GEMSED goed functioneert.

C Beschrijving GEMSED

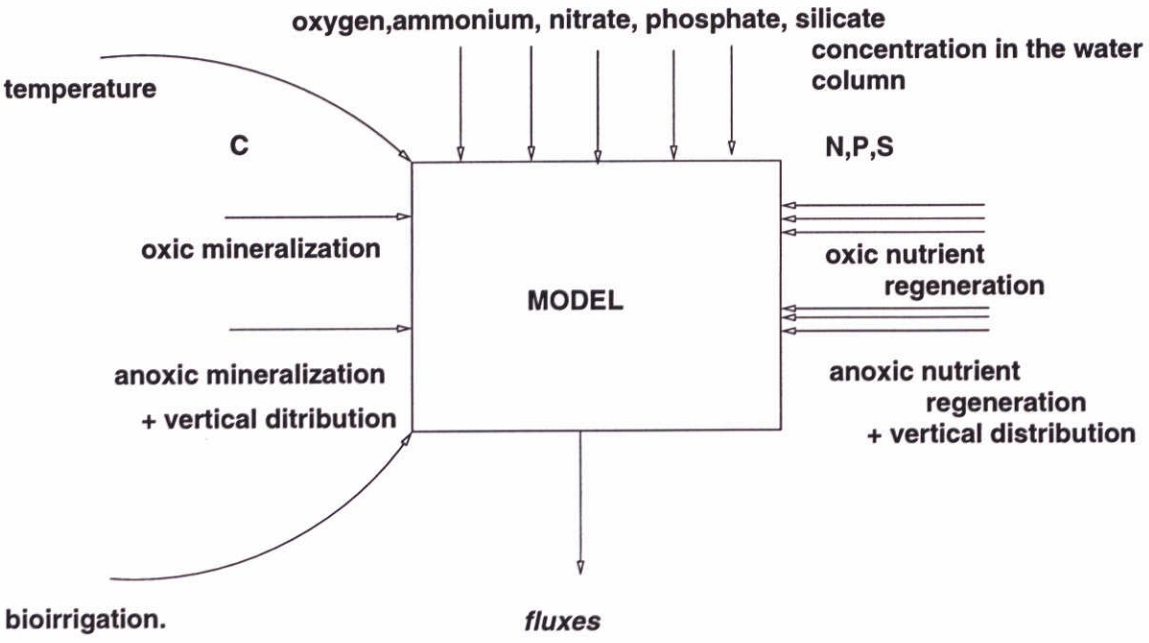

Fig. 1. The input/output information stream into/from the model.

1. SCIENTIFIC DESCRIPTION OF GEMSED

1.1. INTRODUCTION

The benthic nutrient model GEMSED was originally developed for the ERSEM-model (Baretta *et al.*, 1995), with which include all major cycli of all important macronutrients (C,N,P,SI) The present approach concerns a conceptual model with a low number of state variables and parameters, in which only a limited amount of *a priori* knowledge of the processes dominating the benthic system is incorporated. In summary the original aim of this this was twofold:

- to construct nutrient models for the sediments including all important early diagenetic processes for the whole North Sea and describing the direct and indirect effects of the deposition of particulate organic matter on the nutrient cycles in space and time;
- to develop and test a computationally efficient method to model the dynamical behaviour of nutrient pore-water profiles but especially nutrient fluxes.

The input to this submodel is summarized in Fig. 8. The submodel needs in order for the calculation of the profiles the actual values of the mineralizations fluxes (oxic and anoxic), the regeneration fluxes (oxic and anoxic) and N, P and Si. Also it needs a value which describes the vertical exponential distribution of the anoxic mineralizations and regenerations. The model itself calculate only fluxes with which each time step the state variables are updated.

1.2. THE COUPLING OF GEMSED TO GEM

The coupling og GEMSED to GEM is a complicated task. In the first place about 30 values representing state variables, fluxes and forcing are needed to describe the exchange of information

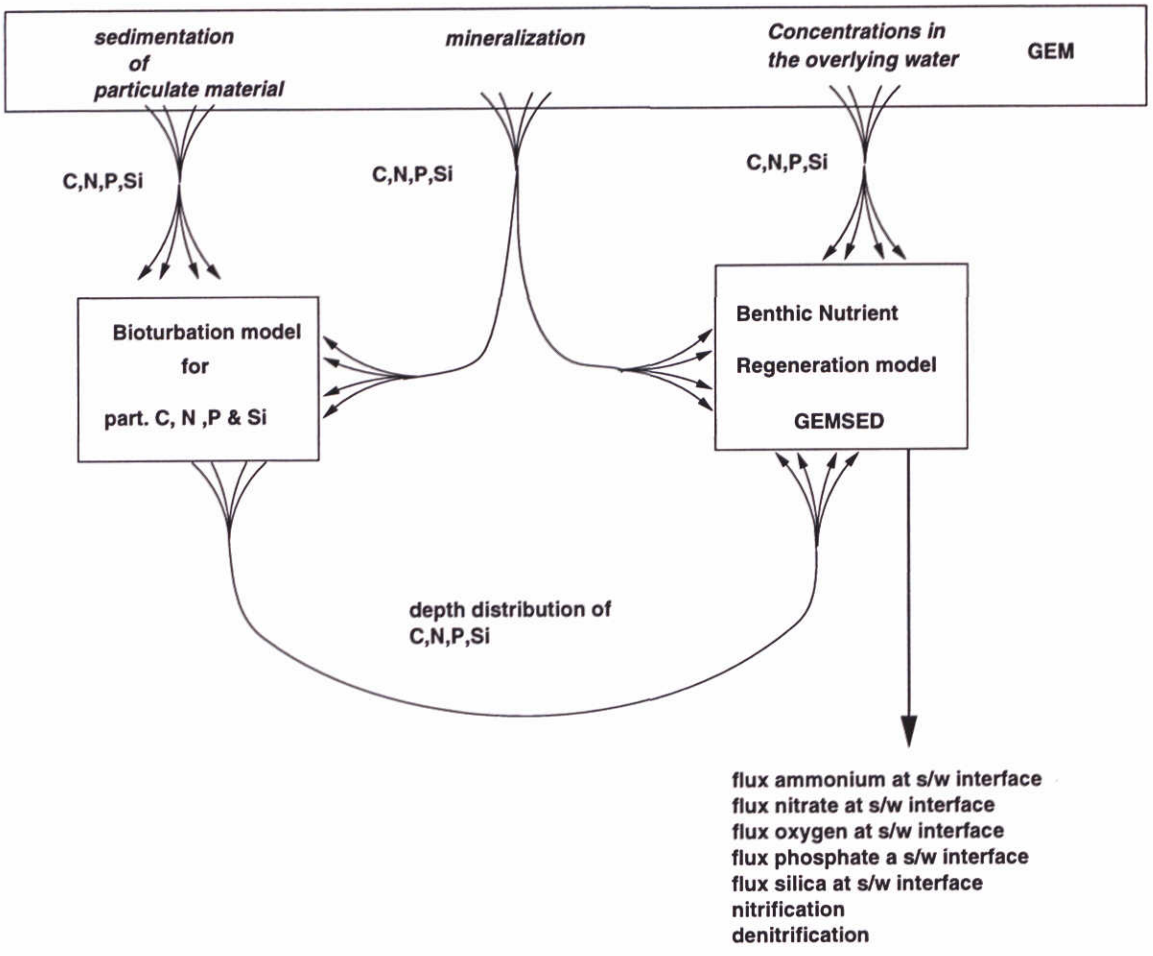

Fig. 2. The detailed representation of coupling between GEM and GEMSED

between GEM and GEMSED and in the second place an auxilarly submodel, also orginating from the ERSEM had to be included describing the transport and reworking of the particulate material by macrobenthos. The necessity for such inclusion follows from the way on which the anoxic mineralization of detritus is formulated in the orignal ERSEM-model In that model the assumption is made that the vertical distribution of the particulate detritus in the sediment is negative exponential. With the (ERSEM-)bioturbation model the variable representing the negative exponent is dynamically modelled for all particulate constituents seperately.

In Fig. 2 the coupling is visualized in tables 1 and 2 detailed lists are given of input and output variables to and from the GEMSED model. With the sedimentation rate in the bioturbation model the depth distribution can be corrected. The same is valid for the mineralization rates, however there the "average" depth where the mineralization take place has to be given as additional information in order to correct the depth distribution in a correct way. Be aware that NOT the concentration of detritus is modelled in the bioturbation model; this one is already present in the GEM model.

Table 1. I/O to/from Benthic nutrient regeneration model

I/O	Type		GEMSED Name	unit
Input	segment-dependent parameters			
	porosity		poro	-
	phosphate adsorp. coef.		pK1_ae	-
Input-rates	oxic mineralization	C	rrBTo	mmol C m^{-2} d^{-1}
		N	reBTn	mmol N m^{-2} d^{-1}
		P	reBTp	mmol P $m^{-2}d^{-1}$
	anoxic mineralization	C	rrATo	mmol C m^{-2} d^{-1}
		N	reATn	mmolN m^{-2} d^{-1}
		P	reATp	mmolP m^{-2} d^{-1}
Input state variables	concentration in the overlying water	O_2	O2o	mmolO_2 m^{-3}
		NH_4^+	N4n	mmolN m^{-3}
		NO_3^-	N3n	mmolN m^{-3}
		PO_4^{3-}	N1p	mmolP m^{-3}
Input forcing	temperature			°C
	depth distribution of	C	*See table 2*	m
	(calculated in	N	*See table 2*	m
	(bioturbation model)	P	*See table 2*	m
Input/Output states variables	in oxic layer	NH_4^+	K4n	mmolN m^{-2} d^{-1}
	in other layers	NH_4^+	K14n	mmolN m^{-2} d^{-1}
	in all layers	NO_3^-	K3n	mmolN m^{-2} d^{-1}
	in oxic + denitrification layer	PO_4^{3-}	K1p	mmolP m^{-2} d^{-1}
	in anoxic layer	PO_4^{3-}	K11p	mmolP m^{-2} d^{-1}
	in oxic + denitrification layer	reduc. equiv.	K6e	mmolS m^{-2} d^{-1}
	in anoxic layer	reduc. equiv.	K16e	mmolS m^{-2} d^{-1}
	in oxic layer	O_2	G2o	mmolO_2 m^{-2} d^{-1}
Output rates	nitrification		jK4K3n	mmolN m^{-2} d^{-1}
	denitrification		jK3G4n	mmolN m^{-2} d^{-1}
	reoxidation of red.equiv.		jK6K7e	mmolS m^{-2} d^{-1}
	flux at water/sediment interface	at		
		O_2	jG2O2o	mmolO_2 m^{-2} d^{-1}
		NH_4^+	jK4N4n	mmolN m^{-2} d^{-1}
		NO_3^-	jK3N3n	mmolN m^{-2} d^{-1}
		PO_4^{3-}	jK1N1p	mmolP m^{-2} d^{-1}
		red.equiv.	jK6N6e	mmolS m^{-2} d^{-1}

1.3. BASIC CONCEPTS

The basis for our models is the general diagenetic equation developed in Berner (1980). For any component dissolved in the pore water this equation takes the form:

$$\frac{\partial \phi C}{\partial t} = \frac{\partial(\phi D \frac{\partial C}{\partial z})}{\partial z} - \frac{\partial(\phi \omega C)}{\partial z} + \phi \Sigma R \qquad (1)$$

Table 2. I/O to/from Bioturbation model (auxilary model)

I/O	Type		Depth	GEMSED Name	unit
Input	particulate sedimentation flux	C	0	psedC	gC $m^{-2}d^{-1}$
		N	0	psedN	mmolN m^{-2} d^{-1}
		P	0	psedP	mmolP m^{-2} d^{-1}
	oxic mineralization	C	average	rrBTo	gC $m^{-2}d^{-1}$
		N	of the oxic layer	reBTn	mmolN $m^{-2}d^{-1}$
		P		reBTp	mmolP $m^{-2}d^{-1}$
	anoxic mineralization	C	average	rrATo	gC $m^{-2}d^{-1}$
		N	of the anoxic layer	reATn	mmolN $m^{-2}d^{-1}$
		P		reATp	mmolP $m^{-2}d^{-1}$
Output	total rate of change of state variable representing depth distribution of	C		D6m	m
		N		D7m	m
		P		D8m	m

where

C: Concentration of the component dissolved in the pore water (mmol·m^{-3}).

t: time (day).

z: depth in the sediment, zero at the sediment-water interface (m).

ϕ: volumetric porosity (-).

D: whole sediment diffusion coefficient ($m^2 \cdot d^{-1}$).

ω: whole sediment advection constant ($m \cdot d^{-1}$).

ΣR: the sum of all reactions and transformations affecting C (mmol·$m^{-3} \cdot d^{-1}$).

All parameters of eq. (1) may vary with depth and can be a function of other components. This implies that eq. (1) represents a set of equations coupled through the parameters. To give an example, NO_3^- production through nitrification is directly coupled to both O_2 and NH_4^+. The vertical variability of the parameters is covered in the models by schematizing the sediment into a limited number of layers. Our main objective is to adequately describe fluxes at the sediment-water interface, rather than to simulate vertical concentration profiles in great detail. Thus we refrain from using a large number of thin layers, but restrict the schematization to three functional layers: 1- the oxic layer, in which O_2 serves as main electron acceptor; 2- the denitrification layer, in which nitrate is reduced; 3- the sulphide layer, in which Mn(IV), Fe(III) and sulphate are reduced through mineralization of organic matter. In each of these layers eq. (1) is applied with depth invariant parameters. The layers are linked by stating continuity in both concentrations and fluxes at the boundaries. The other simplifications are:

- all loss processes are modelled as first-order reactions, productions are assumed to have zero-order kinetics;
- fast adsorption is included as an instantaneous equilibrium reaction (Berner, 1976);

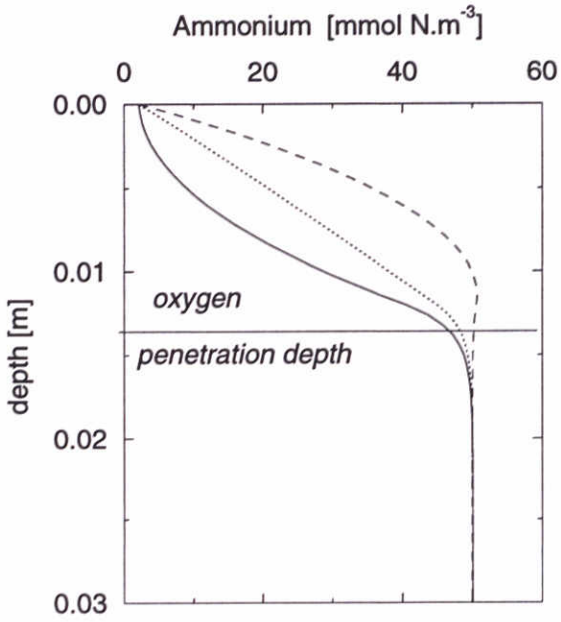

Fig. 3. An example of an initial profile P_{in} (solid line)obtained from the preceding time step, a steady state profile P_{eq} (dashed line) and a transient profile P_{tr} (dotted line) for ammonium. See text for further explanation .

- advection is ignored as relatively unimportant in comparison to diffusion and the other processes concerned.

Now for each of the layers the basic equation becomes:

$$(p+1)\frac{\partial C}{\partial t} = D\frac{\partial^2 C}{\partial z^2} - kC + M \tag{2}$$

in which:

k: first-order loss rate constant (d^{-1}).

M: zero-order production rate constant ($mmol \cdot m^{-3} \cdot d^{-1}$).

p: dimensionless distribution coefficient defined as the proportion between the concentration of the adsorbed and dissolved constituent, respectively.

1.4. SIMULATION OF FLUXES AND GRADIENTS

The model is based on analytical solutions of eq. (2). Obviously, full dynamic solutions of eq. (2) cannot always be found and the approach would then lead to serious mathematical problems. Instead we approximate the dynamical behaviour starting from steady-state solutions of eq. (2). Subsequently we make corrections to account for the effect of changing fluxes and profiles within a time-step. This sequence (steady state, corrections) is performed every time-step of a simulation run. The steady-state solutions are obtained by standard numerical techniques (Press *et al.*, 1986) after introduction of the time-step dependent boundary conditions and parameter values. The need for correction is based on the consideration that it takes some time to reach a new steady state and that steady-state fluxes and profiles may not be established within a single time step. Consequently the steady-state fluxes do not represent time-step averaged fluxes, even when steady-state actually is reached within a time step. The average profiles and hence the time-step dependent fluxes depend

also on the initial profiles. To account for this we distinguish three concentration profiles for each layer (Fig. 3): 1. the initial profile (P_{in}) obtained from the preceding time step; 2. the equilibrium profile (P_{eq}) finally to be obtained at steady-state conditions and 3. the transient profile (P_{tr}) defined as the time averaged profile underway from P_{in} towards P_{eq}. The correction thus consists of calculating P_{tr} and its associated fluxes.

The calculation is done in an indirect way. The associated depth averaged concentrations $\overline{C_{in}}$ and $\overline{C_{eq}}$ are determined from P_{in} and P_{eq}, respectively, and are used to calculate $\overline{C_{tr}}$ according to:

$$\overline{C_{tr}} = \overline{C_{eq}} + (\overline{C_{in}} - \overline{C_{eq}}) \cdot (1 - e^{-\frac{\Delta t}{t_a}}) \cdot \frac{t_a}{\Delta t} \tag{3}$$

in which Δt is the time step and t_a the adaptation time.

From the analytical solution of the general dynamical equation (Carslaw & Jaeger, 1946) the adaptation time (t_a) is derived and is defined as (Ruardij & van Raaphorst, 1995):

$$t_a = \frac{p+1}{k + \pi^2 D/H^2} \tag{4}$$

in which D is the diffusion coefficient in the layer and H is the thickness of the layer in which C is defined Subsequently, P_{tr} is calculated under the constraint that the average value of C is $\overline{C_{tr}}$.

To calculate P_{tr} we assume that changes from time step to time step are small in the deeper layers and that the shapes of the profiles within the individual layers are close to their steady state. In other words, we expect 'pseudo steady state' in the layers, however, without 'equilibrium' between the layers. Thus P_{tr} is calculated from the steady-state solutions of eq. (2), creating a fictitious mineralization term to match $\overline{C_{tr}}$ in the upper layer and P_{in} in both lower layers. From P_{tr} the concentration gradients at the interfaces and associated fluxes are calculated, as well as all first-order loss processes. Subtracting the fluxes and losses from the original and true mineralization yields the total change $\overline{\Delta C}$ in the layers. This value is transferred to the integration subroutine of the simulation package for the calculation of the next $\overline{C_{in}}$ after Δt.

The applied calculation scheme is robust, but gives only acceptable results when the changes ΔC during a time step are not too large. This is extensively tested with the ERSEM-model which make use use of an adaptive time-step algorithm that minimizes the step sizes at large values of ΔC (Ruardij & van Raaphorst, 1995).

Especially in cases of thin layers changes of the input fluxes to the submodel (mineralization fluxes), are directly taken in account by correcting the vertical profile and hence all output fluxes (especially vertical fluxes) are directly adapted to the input.

1.5. THE SUBMODULES

1.5.1. GENERAL

Below we describe the submodules for ammonium, nitrate, phosphate and silica. The interrelations between the different submodules are given in Fig. 4. As mentioned in the introduction, the sediment is divided into three functional layers (oxic layer, denitrification layer and sulphide layer). The depths of the interfaces between these layers are dynamically modelled and are coupled to the diagenetic redox processes. The upper interface is the oxygen penetration depth (z_{ox}). The second

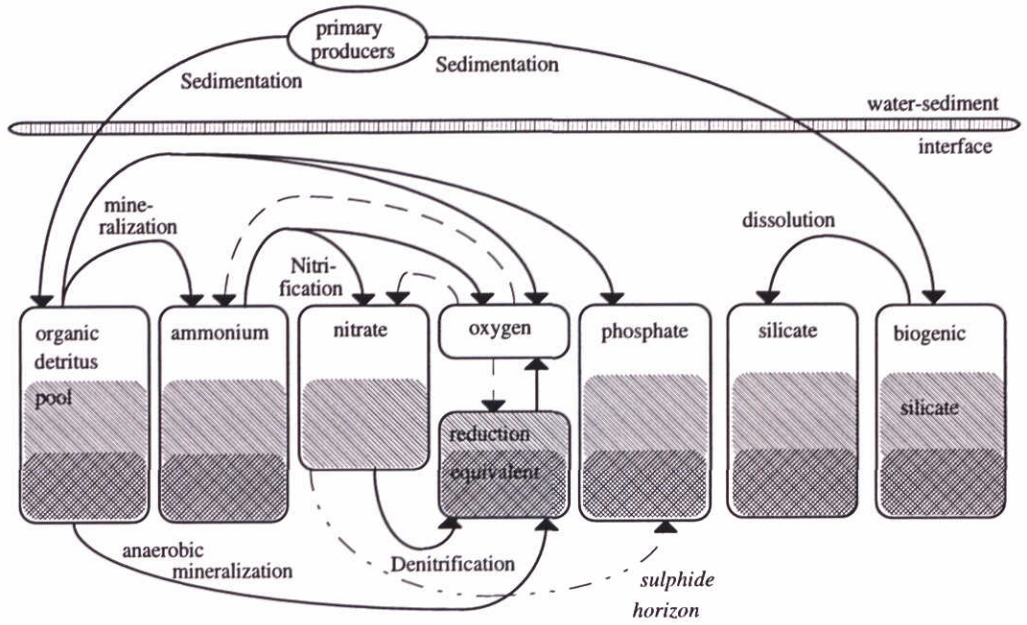

Fig. 4. The interrelations ('arrows') between the different submodules. The input to the benthic system is controlled by the settling of remains of phytoplankton. This input arrives in the benthic organic pool (particulate carbon including N and P) or in the biogenic silica pool. The main driving and controlling force of the benthic nutrient processes is mineralization: phosphate, ammonium, oxygen and reduction equivalents are directly affected. Nitrate is coupled to mineralization through nitrification. The oxygen consumption by mineralization, nitrification and oxidation of reduction equivalents determines the interstitial oxygen concentration and the oxygen penetration depth. The oxygen penetration (dashed lines) modifies the nutrient dynamics considerably. The sulphide horizon depth (dotted- dotted line), derived from the nitrate module controls the adsorption properties of phosphate. Silicate is the only nutrient which is not affected by one of the other variables.

interface, the sulphide horizon (z_{an}) is the depth at which sulphate reduction becomes dominant. In between these surfaces nitrate is assumed to be the main oxidant. Manganese and iron are assumed to occur in their oxidized forms in the upper two layers and in their reduced forms below the second interface. Particularly the reduction of Fe(III) to Fe(II) is important to describe different sorption properties of phosphate in the upper two and in the lower layers. The reduction of electron acceptors and the production of ammonium and phosphate are related to the decomposition of organic matter. Decomposition fluxes are obtained from the decompoition module of GEM (See chapter 6) Other variables directly related to the activity of benthic organisms, such as bioirrigation and bioturbation, are calculated also available in GEM. Burial of organic matter and nutrients is not incorporated in the present GEMSED submodel. In the GEMSED-version of this regeneration model silica is not included. The lack of knowledge about the diagenetic silica processes has lead to the conclusion that the application of this model concept is not useful. Moreover because silica uptake of benthic diatoms is not included (until now) in the orginal ERSEM-version.

t

BOX 1 *Set of equations in the ammonium and nitrate model*

$$(p+1)\frac{\partial A(z)}{\partial t} = D_A \frac{\partial^2 A(z)}{\partial z^2} - kA(z) + M_A \qquad (0 \le z \le z_{ox})$$

$$\frac{\partial N(z)}{\partial t} = D_N \frac{\partial^2 N(z)}{\partial z^2} + kA(z) \qquad (0 \le z \le z_{ox})$$

$$(p+1)\frac{\partial A(z)}{\partial t} = D_A \frac{\partial^2 A(z)}{\partial z^2} + M_A e^{-\alpha\zeta} \qquad (z > z_{ox})$$

$$\frac{\partial N(z)}{\partial t} = D_N \frac{\partial^2 N(z)}{\partial z^2} - d_N N(z) \qquad (z > z_{ox})$$

where:

$A(z)$: ammonium concentration in the pore-water (mmol N·m^{-3}).

$N(z)$: nitrate concentration in the pore-water (mmol N·m^{-3}).

z_{ox}: oxygen penetration depth (m).

$\zeta = z - z_{ox}$ (m).

D_A: whole sediment diffusion constant of ammonium (m^2·d^{-1}).

D_N: whole sediment diffusion constant of nitrate (m^2·d^{-1}).

k: specific nitrification rate (d^{-1}).

d_N: specific denitrification rate (d^{-1}).

M_A: ammonium production through mineralization in the oxic layer (mmol N·m^{-3}·d^{-1}).

α: constant, describing the exponential decrease of mineralization with depth (m^{-1}).

p: adsorption distribution coefficient of ammonium (-).

The equations for each nutrient are linked by stating continuity in the concentration and the flux at $z = z_{ox}$. The boundary conditions are for $z = 0$: $A = A(0)$ and $N = N(0)$ and for $z \to \infty$: $\partial A/\partial z = 0$ and $N(z) \to 0$.

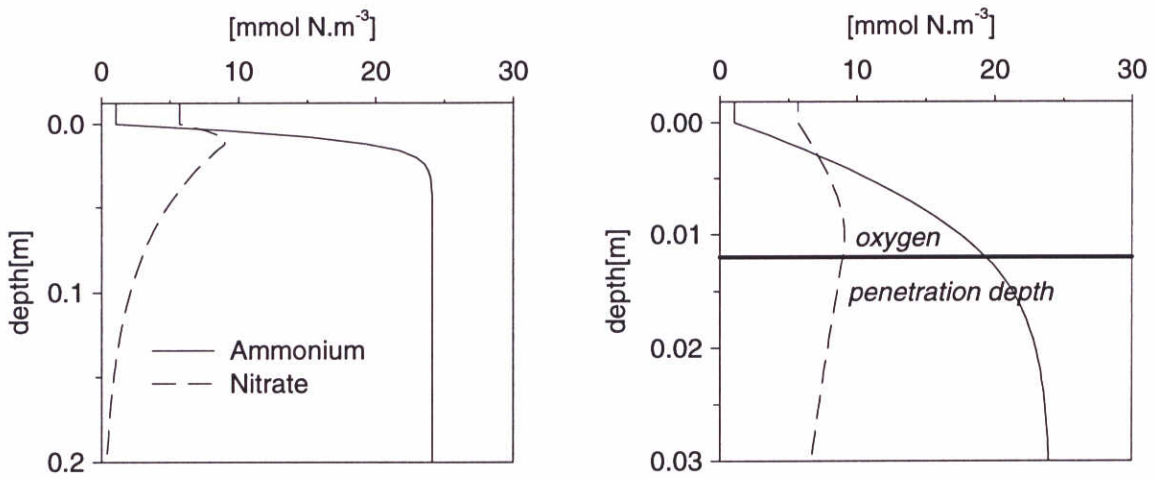

Fig. 5. Steady-state profiles for ammonium and nitrate in the upper 20 cm and upper 3 cm of the sediment obtained from the equations listed in Table 1.

1.5.2. AMMONIUM

Mineralization is the main process controlling ammonium dynamics. Other processes are nitrification, adsorption and of course vertical transport. We apply the steady state model described by Van

BOX 2 *Set of partial differential equations applied for phosphate.*

$$(p_{ox}+1)\frac{\partial P(z)}{\partial t} = D_P\frac{\partial^2 P(z)}{\partial z^2} + M_P \qquad (0 \le z \le z_{ox})$$

$$(p_{ox}+1)\frac{\partial P(z)}{\partial t} = D_P\frac{\partial^2 P(z)}{\partial z^2} + M_P e^{-\alpha\zeta} \qquad (z_{ox} < z \le z_{an})$$

$$(p_{an}+1)\frac{\partial P(z)}{\partial t} = D_P\frac{\partial^2 P(z)}{\partial z^2} + M_P e^{-\alpha\zeta} \qquad (z > z_{an})$$

In these equations:

$P(z)$: phosphate concentration in the pore-water (mmol P·m^{-3} pw).

z_{ox}: oxygen penetration depth (m).

z_{an}: sulphide horizon (m).

$\zeta = z - z_{ox}$ (m).

D_P: whole sediment diffusion constant for phosphate (m^2·d^{-1}).

M_P: phosphate production through mineralization in the oxic layer (mmol P·m^{-3}·d^{-1}).

α: constant, describing the exponential decrease of mineralization with depth (m^{-1}).

p_{ox}: adsorption distribution coefficient of phosphate in the oxic and denitrification layer (-).

p_{an}: adsorption distribution coefficient of phosphate in the sulphide layer (-).

The 3 equations are linked by stating continuity in the concentration and the flux at the interfaces between the 3 layers. The boundary conditions are $z = 0 : P = P(0)$ and $z \to \infty$: $\partial P(z)/\partial z \to 0$.

Raaphorst *et al.* (1990) that in turn is a modification of the models of Vanderborght & Billen (1975) and Vanderborght *et al.* (1977). In their nitrate models Goloway & Bender (1982) and Jahnke *et al.* (1982) assumed that ammonium released during oxidation of organic matter is immediately converted into nitrate when sufficient oxygen is present, without any build-up of reaction intermediates. When describing both nitrate and ammonium, such a rapid conversion is best formulated as a first-order nitrification rate. This approach is further justified by the expected ammonium concentrations in the oxic few upper mm of the sediment in most of the ERSEM-segments ($<$ 25 mmol N·m^{-3}), which are low compared to the half saturation constant for ammonium oxidation (Henriksen & Kemp, 1988). The adsorption of ammonium onto sediment particles by ion exchange reactions is considered a fast process and consequently the ammonium distribution between the solvent (pore water) and the sorbent phase (sediment particles) is assumed to be in equilibrium. The equilibrium distribution is mostly characterized by a linear distribution coefficient (Mackin & Aller, 1984) and is implemented in the model as a reduction of the apparent rate parameters (*e.g.* mineralization, nitrification and diffusion) (Berner, 1976). Following Vanderborght & Billen (1975) the sediments are partitioned in two layers: a nitrification zone extending from $z = 0$ at the sediment surface to the oxygen penetration depth (z_{ox}), and a zone below where nitrification is absent. The ammonium production is described by a zero-order reaction in the upper layer and with a declining exponential term in the lower layer. The set of partial differential equations for ammonium is given in box 1. In Fig. 5 an example of a steady-state ammonium profile is given.

1.5.3. NITRATE

Nitrate is coupled to ammonium through nitrification in the oxic layer. Denitrification is described as a first-order loss process. Steady state models to describe nitrification and denitrification including vertical transports are well-established (Vanderborght & Billen, 1975; Vanderborght *et al.*, 1977;

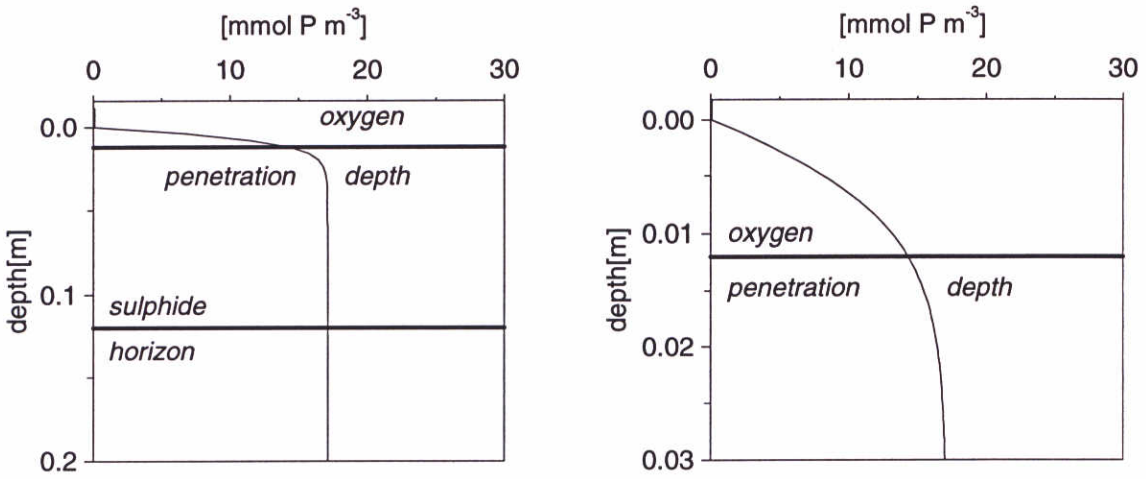

Fig. 6. The steady state profiles for phosphate in first 20 cm and first 3 cm of the sediment.

Van Raaphorst *et al.*, 1990).

The general set of partial differential equations is given in box 1. Fig. 5 gives an example of a steady-state nitrate profile obtained with this set of equations.

1.5.4. PHOSPHATE

Adsorption is an important process in sedimentary phosphate dynamics (Van Raaphorst *et al.*, 1988; Sundby *et al.*, 1992). It is assumed that reduction of Fe(III) concurrently mobilizes Fe(II) and adsorbed phosphate in the sulphide layer. We expect that the nitrate concentration remains sufficiently high in the denitrification layer to inhibit the reduction of Fe(III). Thus it is assumed that the proportion between adsorbed and dissolved phosphate is considerably less (2:1, Krom & Berner, 1980) in the sulphide layer than in the upper two layers (250 to 400:1, see section 1.8.). Sorption of phosphate is considered as a fast process and consequently the phosphate concentration in the solvent phase (pore water) and the sorbent phase (sediment particles) are in equilibrium. The phosphate production in the oxic layer is described as a zero-order reaction declining exponentially below $z = z_{ox}$ and is stoichometrically coupled to the carbon and ammonium mineralization. The set of equations applied in the phosphate submodels is presented in box 2. An example of steady state phosphate profiles obtained with this set of equations is given in Fig. 6.

1.6. REDUCTION EQUIVALENTS

In the North Sea the oxygen penetration in sediments varies from a few mm in coastal to a few cm in off-shore areas (Lohse *et al.*, 1993). Nitrate may penetrate much deeper than oxygen (Jørgensen, 1989; Van Raaphorst *et al.*, 1990). In the reduced sediment below, sulphate reduction mostly is the dominant process in the degradation of organic matter (Froelich *et al.*, 1979). Modelling of the anaerobic oxidation reactions is important for two reasons. First, it is necessary to maintain mass conservation. Second, ions reduced by anaerobic mineralization can substantially add to oxygen

BOX 3 *Set of partial differential equations applied for reduction equivalents.*

$$\frac{\partial R(z)}{\partial t} = D_S \frac{\partial^2 R(z)}{\partial z^2} - r_R R(z) \qquad (0 \le z \le z_{ox})$$

$$\frac{\partial R(z)}{\partial t} = D_S \frac{\partial^2 R(z)}{\partial z^2} + M_o e^{-\alpha\zeta} - \xi_d d_N N(z) \qquad (z > z_{ox})$$

In these equations:

$R(z)$: reduction equivalent concentration in the pore-water(mmol $O_2 \cdot m^{-3}$). = (- O_2concentration in the pore water)

$N(z)$: nitrate concentration in the pore water (mmol $N \cdot m^{-3}$).

z_{ox}: oxygen penetration depth (m).

$\zeta = z - z_{ox}$ (m).

D_S: diffusion coefficient of sulphide ($m^2 \cdot d^{-1}$).

M_o: formation of reduction equivalents through anoxic carbon mineralization (mmol $O_2 \cdot m^{-3} \cdot d^{-1}$).

α: constant, describing the exponential decrease of mineralization with depth (m^{-1}).

r_R: first-order coefficient describing the oxidation of reduction equivalents by O_2 (d^{-1}).

d_N: first-order denitrification rate for oxidation of organic carbon by nitrate (d^{-1}).

ξ_d: denitrification stoichiometric factor (= 0.3 mmol $O_2 \cdot$ (mmol N)$^{-1}$).

M_r is unknown and calculated from the steady-state solution. The two equations are linked by stating continuity in the concentration and the flux at $z = z_{ox}$. The boundary conditions are $z = 0$: $R = 0$ and $\partial R/\partial z = 0$ and $z \to \infty$: $\partial R/\partial z \to 0$.

BOX 4 *Set of partial differential equations for oxygen.*

$$0 = D_{Ox} \frac{\partial^2 Ox(z)}{\partial z^2} - M - \eta_r M_r - M_n \qquad (0 \le z \le z_{ox})$$

$$z_{ox} = \sqrt{\frac{2DOx_0}{M + \eta_r M_o + M_n}}$$

$$z_{an} = \log 0.10 / \sqrt{d/D_N} + z_{ox}$$

in which:

Ox: O_2 (mmol $O_2 \cdot m^{-3}$).

z_{ox}: O_2 penetration depth (m).

z_{an}: sulphide horizon (m).

D_{Ox}: diffusion constant of oxygen ($m^2 \cdot d^{-1}$).

D_N: diffusion constant of nitrate ($m^2 \cdot d^{-1}$).

M: zero-order O_2 consumption rate (mmol $O_2 \cdot m^{-3} \cdot d^{-1}$).

M_r: zero-order oxidation rate of reduction equivalents (mmol $S^{2-} \cdot m^{-3} \cdot d^{-1}$).

η_r: O_2:S^{2-}conversion factor (=2 (mmol O_2)$\cdot$(mmol S)$^{-1}$).

d: denitrification constant (d^{-1}).

M_n: average nitrification rate (mmol $O_2 \cdot m^{-3} \cdot d^{-1}$). Defined as:

$$M_n = \frac{\xi_k k}{z_{ox}} \int_{z=0}^{z_{oz}} A(z) dz$$

k: nitrification constant (d^{-1}).

ξ_k: nitrification stoichiometric factor (= 2 mmol $O_2 \cdot$(mmol N)$^{-1}$).

$A(z)$: NH_4^+ concentration (mmol $N \cdot m^{-3}$).

The boundary condition for the equation are $z = 0$: $Ox = Ox(0)$ and $z \ge z_{ox}$: $Ox(z) = 0$.

demands in the oxic sediment layer and thus influence the oxygen penetration depth (Billen, 1982). Oxidation of reduced components as Fe(II), Mn(II) or HS^- may even dominate oxygen consumption rates at specific locations during certain periods in the seasonal cycle (Canfield *et al.*, 1993).

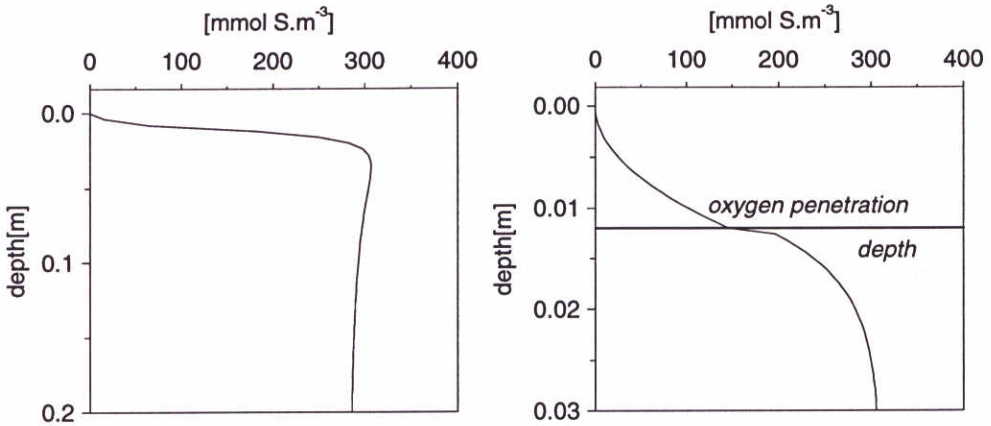

Fig. 7. Steady-state profile for reduction equivalents in the upper 20 cm and upper 3 cm of the sediment.

Modelling of all the redox elements explicitly is not necessary, however, for our purpose. Instead we make use of the negative oxygen concentration as modelled in GEM representing all reduced components except nitrate generated in the denitrification and sulphide layer. This negative concentration can be considered as a pool of reduced ions with the properties of the most common one, sulphide (*e.g.* diffusion coefficient). The reduction equivalents diffuse upward towards the oxic layer where they are oxidized by O_2, we assume that they are not oxidized by NO_3^-. The oxidation rate M_r is determined from the additional boundary condition $\partial R/\partial z = 0$ at $z = 0$. The general set of partial differential equations applied to reduction equivalents is given in box 3. Examples of steady-state profiles obtained with this set of equations are given in Fig. 7.

1.7. OXYGEN PENETRATION DEPTH AND SULPHID HORIZON

The oxygen penetration depth (z_{ox}) and the depth at which the sulphate reduction starts (z_{an}) have to be known before the nutrient equations can be solved. Mineralization of organic matter is the main O_2-consuming process, but nitrification and oxidation of reduced ions can enhance the O_2 consumption considerably. We apply the model of Bouldin (1968) to calculate the O_2 profiles and penetration depths (box 4). In contrast to Bouldin (1968), however, we included zero-order consumption rates to take nitrification and oxidation of reduction equivalents into account. The interface between the denitrification layer and the sulphide layer (z_{an}), called the sulphide horizon, is derived from the nitrate submodel. The nitrate gradient shows an exponential decrease with depth due to denitrification below z_{ox} (Fig. 5). Following the criterion of Van Raaphorst *et al.* (1990) we defined the sulphide horizon (z_{an}) as the depth at which denitrification has decreased to 10% of its initial value at the oxygen penetration depth (box 4).

1.7.1. BIOTURBATION- DEPTH PROFILES OF DETRITUS DENSITIES

Each detritus component in the ERSEM model on which this GEMSED model is based is described by the mass but also by a state variable which describes the vertical distribution. This vertical distribution is assumed to be exponential and hence the state variable describes the mean intrusion

Table 3.
Overview of the input variables into the benthic nutrient model.

variable	*variable type*	*calculated in submodel*
P-mineralization	rate	benthic biology model
N-mineralization	rate	benthic biology model
O_2-mineralization	rate	benthic biology model
temperature	forcing function	
bioirrigation	environmental variable	benthic biology model
porosity	environmental variable	parameter

depth of component into the sediment. The main purpose in ERSEM however was the modelling in a simple way of the bioturbation. In this way microbiological activity and nutrient production by decomposition will depend on detritus density and composition at different depths. The GEMSED-version of this (bioturbation) submodel in the GEM-environment aims only to estimate the intrinsic depth from the particulate transport dynamics in the sediment as modelled in GEM. Therefore in the GEM-model on all places where rates are calculated modifying the concentration of particulate marerial an extra rate definition has to be defined with which the total change of the intrinsic depth can be derived:

$$\Delta D_i = (d - D_i)\frac{f}{\Sigma Q} \tag{5}$$

in which:

D_Q: the intrinsic depth of particulate constituent Q (m)

ΔD_Q: Rate of change of D_Q (m d^{-1})

d: Everage depth at which change in Q take place (m).

f: Rate of change of Q (mg $m^{-2}d^{-1}$).

ΣQ: Total amount of Q present in the sediment(mg m^{-2}).

1.8. External forcing

The forcing parameters are divided in 2 groups. The first group consists of parameters which are calculated outside the nutrient submodels and from there are introduced into the benthic nutrient submodels (Table 3). All mineralization rates are within this group of external parameters. The second group of parameters is specified in the benthic nutrient submodels. These parameters may be corrected for temperature, bioirrigation and porosity of the sediments. The latter three variables are either taken as forcing functions from outside the ERSEM model, or are calculated in the benthic biology model (Ebenhöh *et al.*, 1995).

The main source of organic matter to the benthic system is detritus, generated in the pelagic system and deposited on the sea floor or filtered by suspension feeders. Subsequently the detritus

is redistributed in the sediment by particulate transport and bioturbation and decomposed by benthic organisms. All these processes are described in the benthic biology model. In our model it is assumed that the detritus is exponentially distributed with depth. The steepness of this exponential distribution is recalculated from the output of the benthic biology model. The decomposition of organic matter in the benthic biology model is effectuated by bacteria and macro benthos which consume detritus for their growth. In the benthic biology model it is assumed that all benthic organisms live in the oxic layer. For the thickness of this layer the value of z_{ox} from the previous time step is used. The total mineralization in the oxic layer is derived from the sum of all respirations (O_2) and all excretions (N and P) of the benthic organisms in this layer. In the other layers the mineralization is caused by the activity of anaerobic bacteria. These mineralizations are the main input to the benthic nutrient model. The parameter α is calculated from the difference between the oxic and anoxic mineralizations (see Boxes 1, 2 & 3):

$$M = \frac{\overline{\mathcal{M}}}{\alpha \cdot H}(1 - e^{-\alpha H}) \tag{6}$$

where M is the average mineralization in the oxic layer (mmol·m^{-3}·d^{-1}), $\overline{\mathcal{M}}$ is the depth-averaged mineralization in the in the layers below $z = z_{ox}$ (mmol·m^{-3}·d^{-1}) and H (=0.3$-z_{ox}$) is the thickness of the 2 lower layers (m).

The physical characteristics of the sediments in the GEMSED segments are important factors for the diagenetic processes in the sediments. In table 1 two parameters can be found which are segment dependent: the porosoty (fraction of water in the sediment) and the adsorption capacity of the sediment for phosphate to iorn. Pororsity and sedimentary contents of reactive components as *e.g.* Fe are in field observations often correlated with grain size distribution (Mackin & Aller, 1984; Wiesner *et al.*, 1990). If not values are availble for these parameters for all segments in the ERSEM the values for these parameters were derived from observations on the weight fraction of particles with the grain size smaller than 63 μm in the sediment:

$$\phi = 0.38662 + 0.0425 p_s \tag{7}$$

$$k_d = 4.031 p_s \tag{8}$$

$$p_p = k_d \frac{(1-\phi)}{\phi} \rho \tag{9}$$

in which

p_s: fraction of sediment with grain szie $< 63\mu$m

ϕ: porosity

k_d: adsorption coefficient (ml/mg)

p_p: adsorption distribution coefficient (-)
(=dimensionless adsorption coefficient)

ρ: density of sediment particles (g m^{-3})

These correlations were found in a large dataset collected in the sediments of the North Sea.

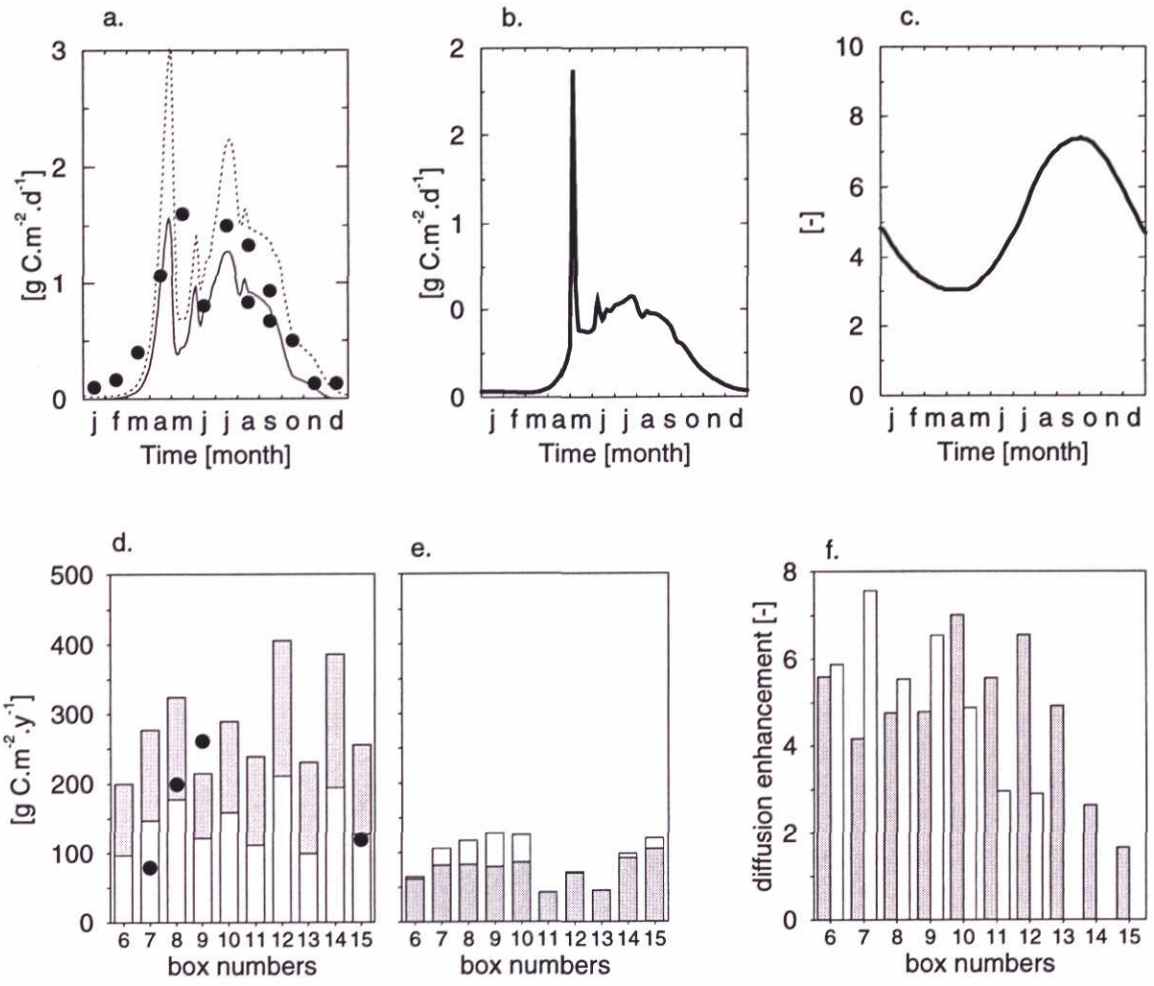

Fig. 8. a. The gross (solid line) and net (dotted line) primary production modelled with the ERSEM model for box 9 and field observations (•) of Joint & Pomroy (1993); b. The seasonal dynamics of deposition of organic material on the sea floor in box 9; c. Yearly variation of the bioirrigation factor C_B (eq. (??)) in box 9 as calculated by the benthic biology model (?); d. Simulated annual gross (white+grey) and net (white) primary production based in the total water column above the sediment of the boxes and primary production based on field observations (•, Joint & Pomroy (1993)); e. Yearly input of organic carbon through sedimentation (grey) and through filtering of suspension feeders (white); f. Annual mean value of the bioirrigation C_B (grey) and of bioturbation factor (white). The latter value is given for completeness only and controls the vertical transport of particulate detritus and silica (?).

2. Description of the results of the model in its orginal ERSEM set-up

2.1. Input to the benthic nutrient model

All results were obtained by running the full ERSEM-model. The primary production (Fig. 8a), deposition of organic carbon (Figs. 8b and 9) on the sediment and the coupled mineralization (Fig. 9) show distinct seasonal dynamics . Most of the sedimented material originates from local primary production. Estimation of primary production from ^{14}C-incubations yields a value somewhere be-

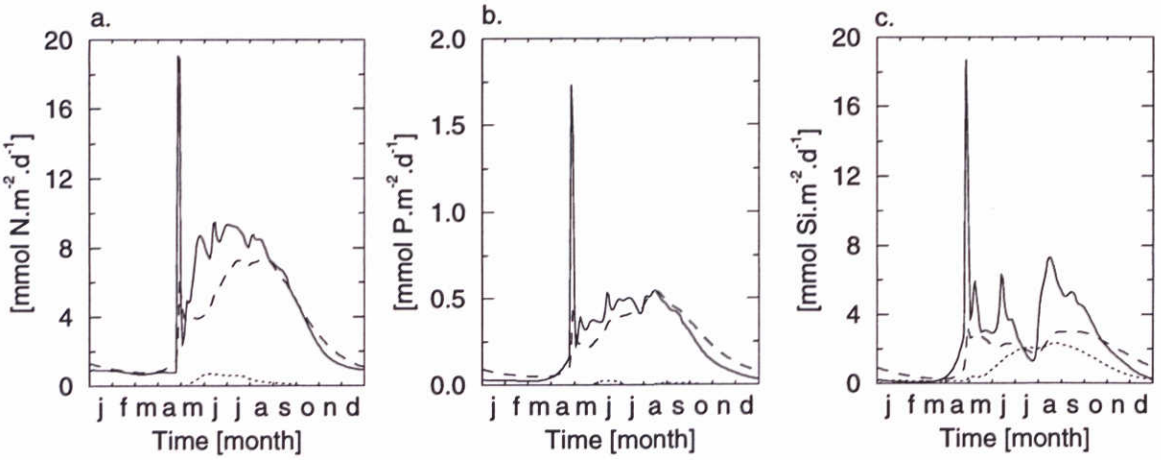

Fig. 9. a. The particulate input (solid line), the mineralization in the oxic layer (dashed line) and mineralization in the lower layers modelled with the ERSEM model in box 9 for nitrogen; b. for phosphate; c. for silicate.

tween gross and net production (Peterson, 1980). Indeed, the primary production data of Joint & Pomroy (1993) are in between simulated net and gross production (Figs 8a and 8d). The resulting mineralization of particulate nutrients is used as input to the benthic nutrient model for the oxic layer and for the lower layers (Fig. 9). For N and P the Benthic Biology model calculates that the largest part of the mineralization takes place in the oxic layer. This is not only explained by the deposition of fresh detritus on top of the sediments. Also, the benthic fauna is assumed to feed in deeper layers and to excrete the excess of nutrients from the consumed detritus and bacteria in the oxic layer. Consequently, there is an upward transport of nutrients associated with the activity of the benthic fauna in the model. Silica dissolution occurs at a slower rate than mineralization of N and P, and which is not affected by ingestion by benthic fauna is distributed deeper into the sediment column.

The bioirrigation factor is estimated from the activity and the biomass of macrobenthos and shows highest values in late summer and lowest just before sedimentation of the spring bloom (Fig. 8c). For details refer to ?). A remarkable result is that a large sedimentation (*e.g.* box 14 and 15) does not necessarily lead to a large bioirrigation (Fig. 8f). Fig. 8d shows that the lowest input of organic carbon to the sea floor is in the boxes 11 and 13.

2.2. PORE-WATER GRADIENTS AND FLUXES

2.2.1. OXYGEN

The model calculates benthic nutrient dynamics in ten different areas for a full annual cycle. To keep the number of results to be presented within reasonable limits, we will focus the discussion on the boxes 9 and 11. Box 9 represents the fully mixed coastal box in the German Bight with large nutrient inputs from the rivers. Box 11 is the lower box in the stratified part in the northern North Sea. Deposition of algal material directly after the spring bloom resulted in a short peak in the benthic oxygen consumption in box 9 (Fig. 10b). Similar peaks were calculated for the other shallow boxes

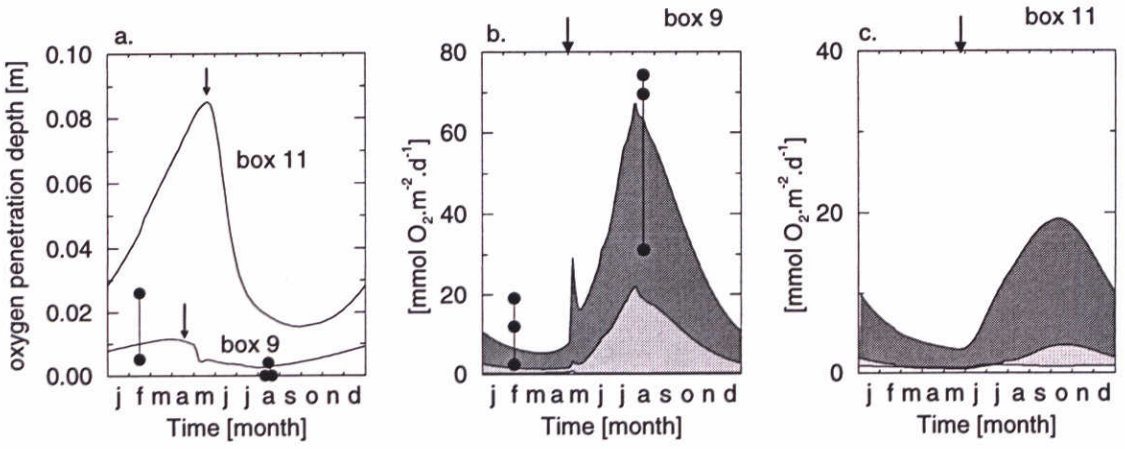

Fig. 10. Seasonal variation of oxygen penetration depth (a), the total oxygen consumption and the contribution of the three oxygen consuming processes in the boxes 9 (b) and 11 (c) respectively: nitrification (white), oxidation of reduced materials (grey) and oxidation of organic material (dark grey). The arrows refer to the maximum of the spring bloom as simulated by the pelagic submodel (Varela *et al.*, 1995). The •'s refer to field observations by Lohse *et al.* (1993) at three stations in the German Bight (box 9).

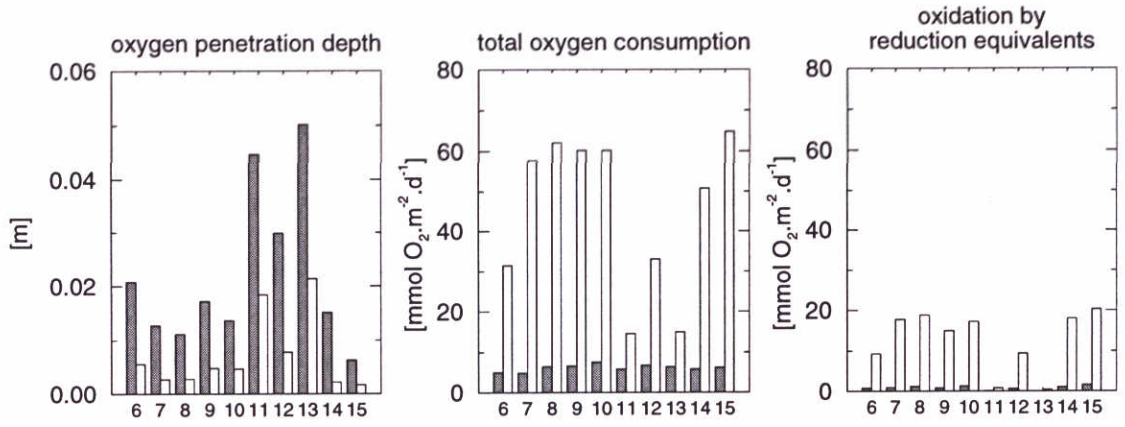

Fig. 11. Annual mean oxygen penetration depths (a), total oxygen consumption (b) and oxygen consumption due to oxidation of reduced material (c) for the month February (dark grey) and the month August (light grey).

(<30 m), but not for the boxes in the deeper parts of the North Sea (*e.g.* box 11). The maximum consumption rates were calculated from August (box 9) to October (box 11). These maxima are related to the deposition of detritus and to high temperatures during summer. Oxygen penetration depth is inversely coupled to the O_2 consumption and consequently shows an inverse seasonal pattern with the highest values just before the spring bloom and lowest in summer (Fig. 10a.).

The proportion between aerobic and anoxic mineralization is controlled by the penetration depth of oxygen (Fig. 11a.) and the total mineralization of organic matter. In box 9 oxygen consumption by nitrification is negligibly small, but 30-40% of the oxygen consumption during summer is used for oxidation of reduction equivalents diffusing upwards from the deeper layers (Fig. 10b). In the

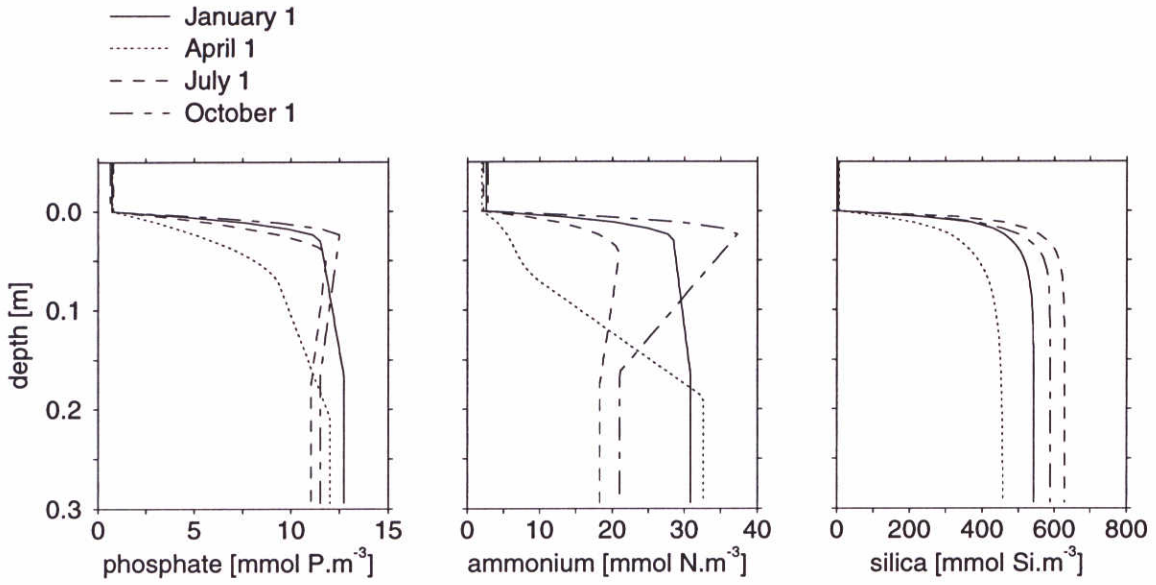

Fig. 12. Profiles for phosphate, ammonium and silica on 4 points in time as simulated for box 9.

deeper box 11, nitrification forms a slightly more substantial part of the oxygen budget. Oxidation of reduction equivalents is less important in the boxes 11 and 13 than in the other boxes. In general the contribution of oxidation of reduction equivalents is most important in summer (Fig. 11c). Primary production in the deeper northern boxes (box 6, 11, 12 and 13) and the deposition of organic material onto the sediment is distinctly lower than in the other boxes (Fig. 8c). This is reflected in the total benthic oxygen consumption (Fig. 11b). The central boxes (14 and 15) have similar oxygen consumption rates as the adjacent coastal boxes with large river inputs (box 7, 8, 9).

2.2.2. AMMONIUM AND NITRATE

The ammonium profiles respond to changes in the ambient circumstances during the year (Fig. 12). The subsurface maxima of the calculated ammonium profiles of box 9 reflect to steady-state conditions in summer and autumn due to the deposition of detrital material. The April profile just before the deposition of the spring bloom represents a situation with low ammonium production and depressed ammonium concentration in the oxic layer caused by nitrification. The seasonal development of the nitrate profiles shows large differences between box 9 and 11 (Fig. 13). In box 9 nitrification causes maximum concentration at 1 to 3 cm depth just before deposition of the spring bloom when oxygen penetration depth is at maximum. From July to September nitrate is almost absent in the pore waters of this box. In box 11 highest nitrate concentrations are calculated for June-July when nitrification is stimulated by increasing ammonium production rates at still large enough oxygen penetration depths. According to the model nitrification is oxygen-limited in the coastal boxes and ammonium-limited in the northern boxes close to the ocean during summer.

In general the calculated concentrations of ammonium in the upper 5 cm agree fairly well with field data (Lohse *et al.*, 1993; Van Raaphorst *et al.*, 1990). Larger discrepancies between simulated

Fig. 13. Seasonal dynamics of profiles of nitrate as simulated respectively for box 9 (left) and box 11 (right).

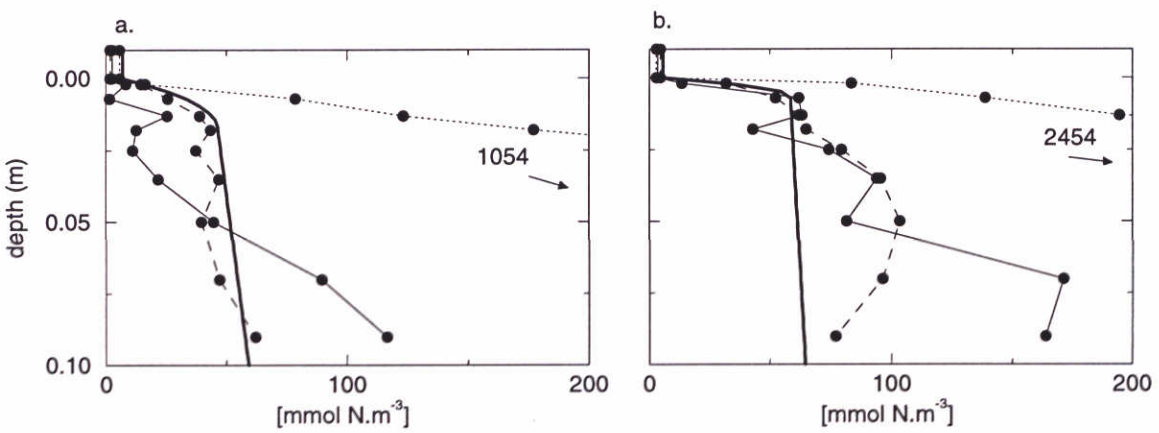

Fig. 14. Simulated NH_4^+ profiles (thick solid line) and measured NH_4^+ profiles at 3 stations (thin solid, dotted and dashed lines) for box 9 in February (a) and in August (b). (Data from Lohse *et al.*, 1993).

and observed values occur in the deeper layers, particularly during summer. An example for box 9 is presented in Fig. 14. The February profile of nitrate (Fig. 15) is within the range of the field data. In August the observed nitrate profiles are lower than the simulated profiles probably due to the higher simulated nitrate concentrations in overlying water. The examples in Figs. 14 and 15 demonstrate substantially different profiles measured within a single ERSEM box. This makes it almost impossible to fully compare the model with field observations.

The sediment-water exchange rates of dissolved nitrogen show a pronounced seasonal variation (Figs. 16 and 18). The fluxes of nitrate and N_2 are suppressed in favour of ammonium during summer. The N_2 flux shows a similar pattern as nitrate, because the main source for denitrification is nitrate produced through nitrification. Nitrate and N_2 fluxes are at maximum in spring when O_2 penetrates deepest into the sediment. In April nitrate and N_2 contribute 25% and 85% to the total N flux in the boxes 9 and 11, respectively (Fig. 16).

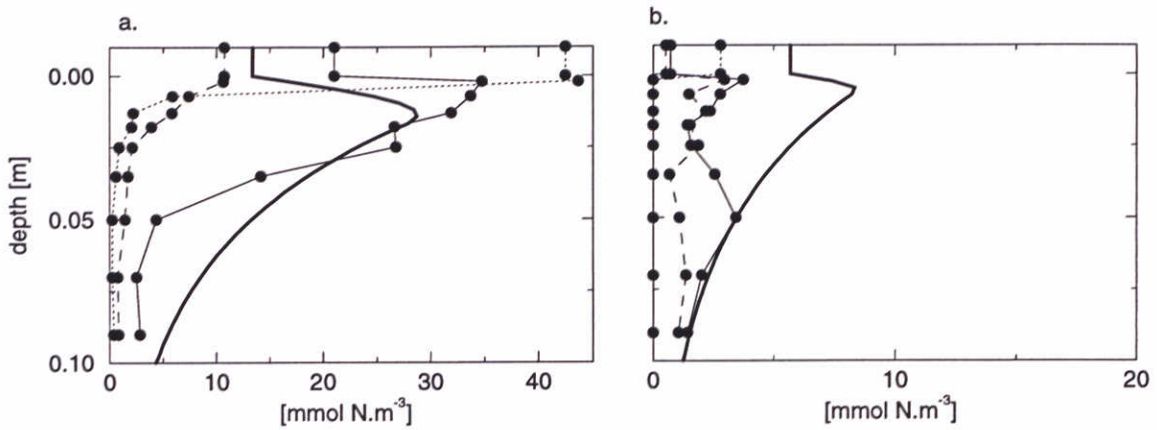

Fig. 15. Simulated NO_3^-profiles (thick solid line) and measured NO_3^-profiles at 3 stations (thin solid, dotted and dashed lines) for box 9 in February (a) and in August (b). (Data from Lohse *et al.*, 1993).

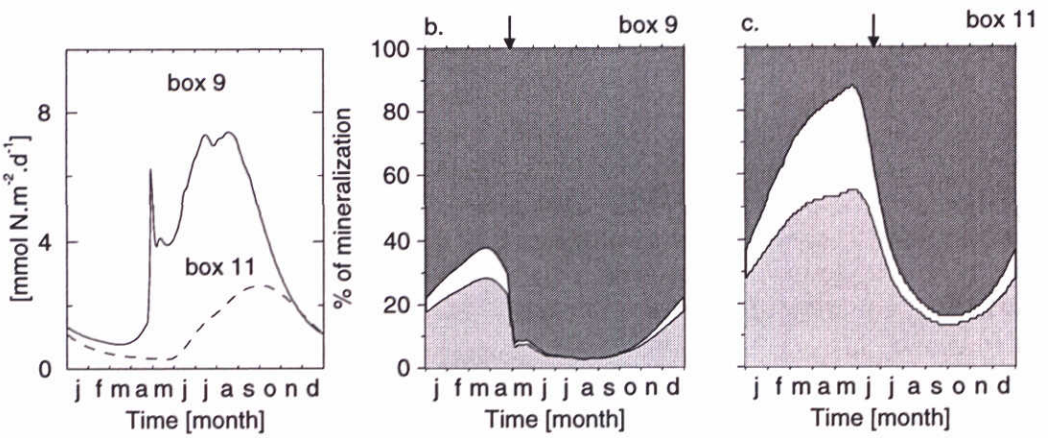

Fig. 16. a: Mineralization of N in box 9 and 11 (mmol $N \cdot m^{-2} d^{-1}$); b: the relative composition of sediment-water fluxes of nitrogen: ammonium (dark grey),N_2 (white) and nitrate (grey) for respectively box 9 and c. idem for box 11. The arrows refer to the maximum of the spring bloom as simulated by the pelagic submodel (Varela *et al.*, 1995).

Substantial parts of the ammonium produced through mineralization are nitrified to nitrate and subsequently denitrified. This holds particularly for the off-shore boxes (11, 12 and 13) during winter. This result is in accordance with field observations of Van Raaphorst *et al.* (1992) and Lohse *et al.* (1993) who concluded that nitrification and denitrification can dominate N-fluxes in non-eutrophied off-shore sediments and that ammonium fluxes dominate in eutrophic coastal areas.

The simulated N-fluxes are compared with field observations of Lohse *et al.* (1993) in Fig. 18. Again, the observations show large variations for most of the measured rates at different stations, demonstrating major heterogeneity within the ERSEM boxes. in the field data.

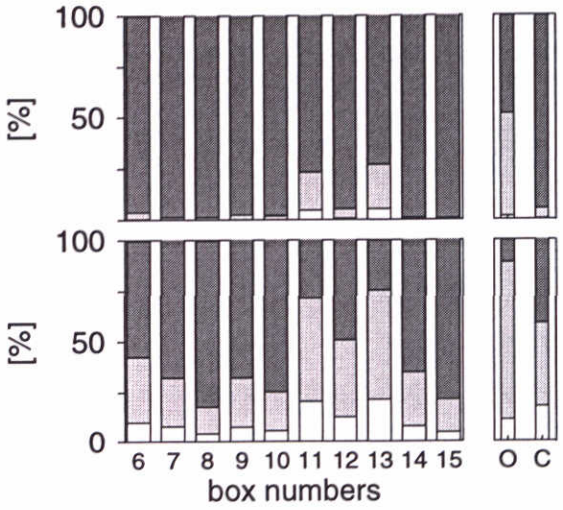

Fig. 17. Simulated annual relative simulated rates of N-mineralization (=100%), nitrification (white +light grey) and denitrification (white) compared with field data of Lohse *et al.* (1993) for offshore (o) and coastal (c) areas for February (lower graph) and August (upper graph).

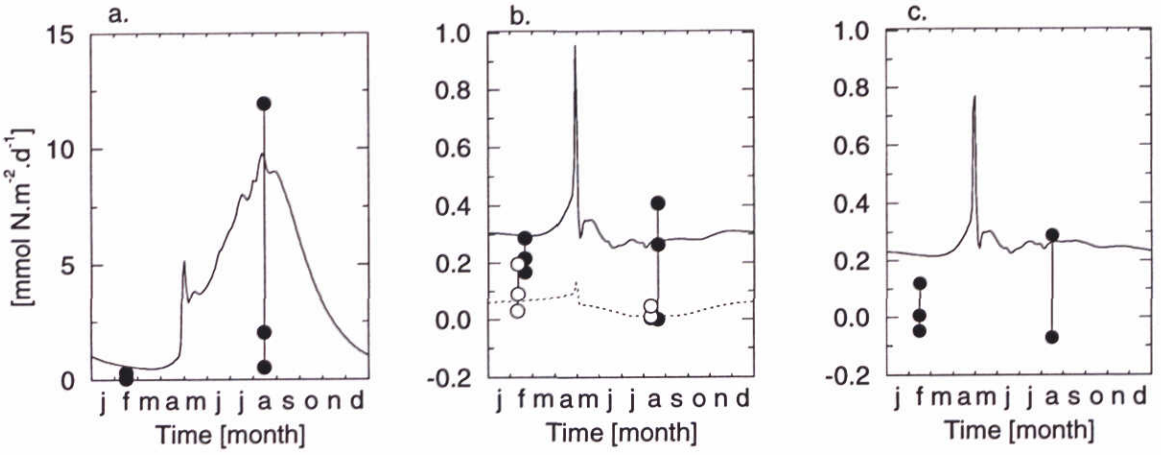

Fig. 18. Simulated seasonal dynamics of the N-fluxes for box 9 with field observations at three stations in the German Bight (•, Lohse *et al.* (1993)). a. Ammonium flux; b. Nitrification (solid line •) and denitrification (dotted line, o) and c. Nitrate flux

.

2.2.3. PHOSPHATE

Production of phosphate and nitrogen is coupled to mineralization of organic carbon. Phosphate shows similar pore water profiles as ammonium (Fig. 12). The low phosphate concentrations in the upper 5 mm, which are observed in February, are, however, not simulated by the model (Fig. 19a). The high pore-water concentrations observed at 2 stations in August are not reproduced by the model (Fig. 19b).

Subsurface gradients of phosphate are less pronounced than those of ammonium (Fig. 12). This is caused by the high adsorption distribution coefficient applied in the phosphate submodel, by which changes in phosphate concentration are buffered in the oxic layer. Fig. 20c indicates that the sorbed pool is largest in summer, but that phosphate is not stored over the season. This is also

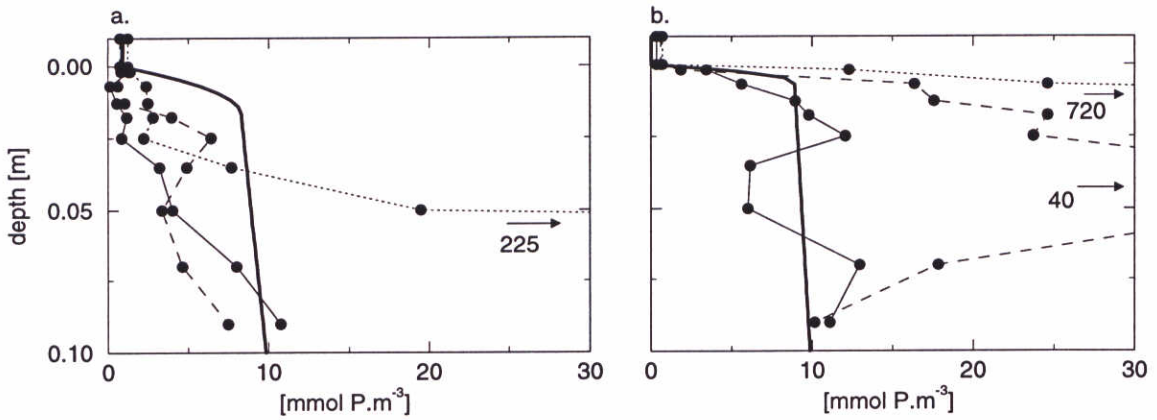

Fig. 19. Simulated phosphate profiles (thick solid line) and measured phosphate profiles at three stations (thin solid, dotted and dashed lines) for box 9 in February (a) and in August (b) (data from SLOMP, unpublished data).

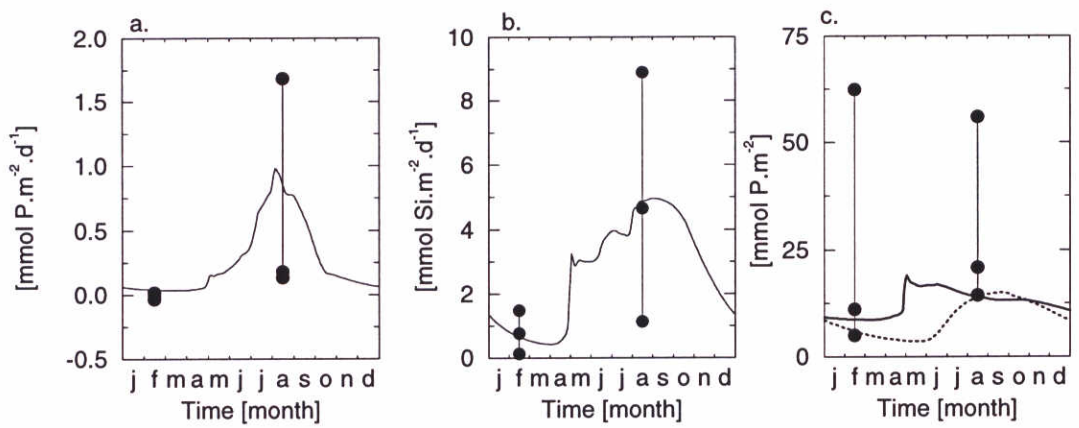

Fig. 20. a. Simulated seasonal dynamics of the P-flux; b. idem for Si-flux for box 9 with field observations at three stations in the German Bight; (•,field data from Slomp & van Raaphorst, 1993a; Gehlen, 1993). c. Simulated seasonal dynamics of phosphate adsorbed in the upper 1 cm of the sediments for box 9 (solid line) and box 11 (dotted line) with field observations at 3 stations in the German Bight (Slomp), unpublished results).

reflected by field observations (Slomp & van Raaphorst, 1993a), especially if the (highest) values measured at Helgoland Bight are neglected as not representative for the entire area (Lohse *et al.*, 1993).

The simulated fluxes of phosphate are within the range as found by Slomp & van Raaphorst (1993b).

2.2.4. SILICATE

The pore-water concentrations are lowest in April just before the deposition of the spring bloom. Highest concentrations are simulated for August-October (Fig. 12) The model did not reproduce the observed profiles in box 9 (Fig. 21). In general, the model calculates too high concentrations in the deeper layers of the sediment. The gradients at the sediment water interface and the simulated

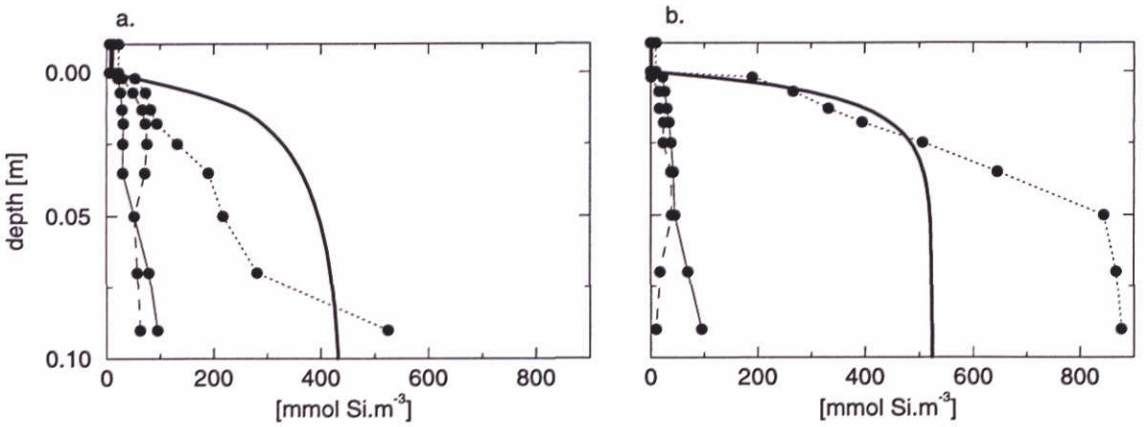

Fig. 21. Simulated silicate profiles (thick solid line) and measured silicate profiles at 3 stations (thin solid, dotted and dashed lines) for box 9 in February (a) and in August (b). (Data from Gehlen, 1993).

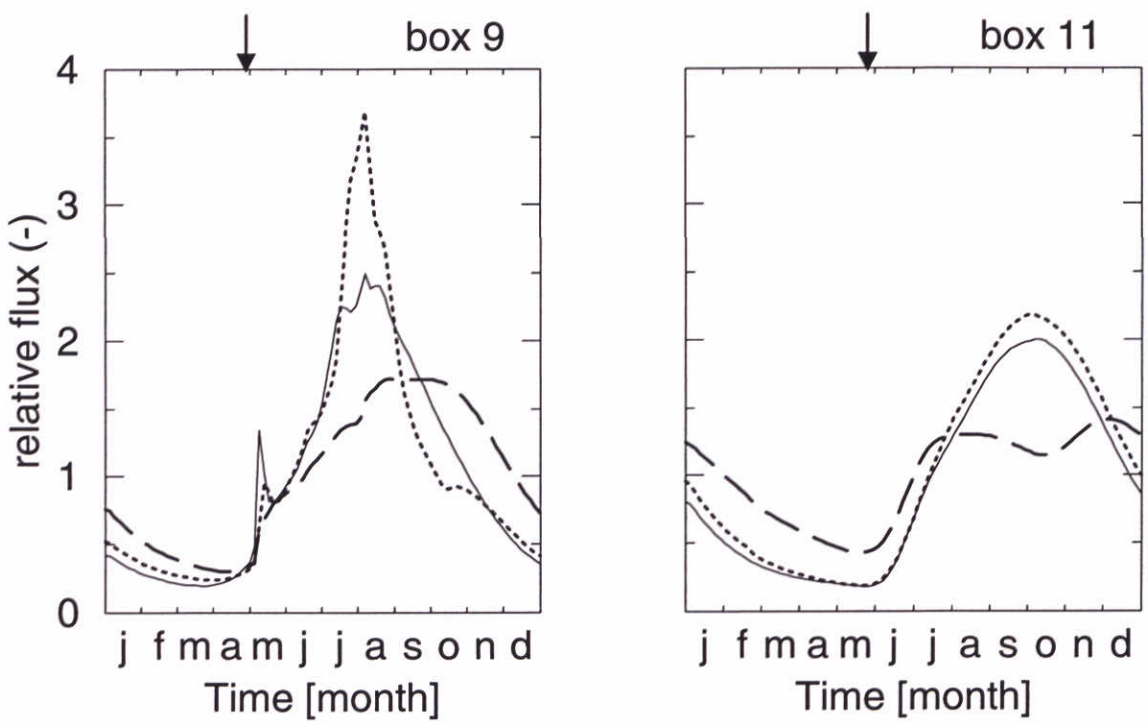

Fig. 22. The relative fluxes of N (solid), P (dotted) and Si(dashed) at the sediment-water interface for box 9 and box 11. The relative fluxes are calculated by dividing the actual flux by the yearly averaged mineralization in the sediment. The arrows refer to the point in time of the maximum of the spring bloom as simulated by the pelagic submodel.

fluxes, however, fit fairly well with the field observations (Fig. 21).

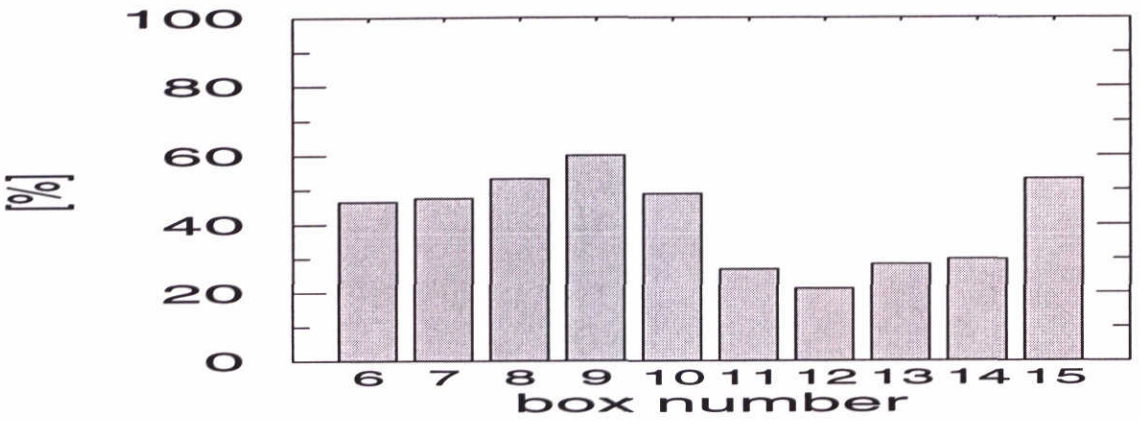

Fig. 23. The percentage of nitrogen taken up by primary producers and mineralized by the benthic system in the ERSEM-boxes.

3. DISCUSSION THE MODEL RESULTS IN ITS ORGINAL ERSEM SET-UP

Early diagenesis of nutrients is driven by mineralization of organic matter in the sediments (Froelich *et al.*, 1979). As a consequence modelling of benthic nutrient dynamics heavily depends on an accurate estimate of the deposition of organic matter on the sea floor. Also the quality of the organic matter in terms of degradability and carbon: nutrient ratios is of importance (Berner, 1980). In the present study deposition and organic matter composition are obtained from other submodels of the ERSEM model and not directly from field data. This means that our results depend on the other ERSEM submodels including their underlying assumptions and simplifications as well as the associated uncertainties and errors. The advantage of this approach, however, is that the interactions between different compartments of the North Sea ecosystem can be evaluated within one single modelling framework (?), and that first estimates on the contribution of the sediments in overall nutrient cycling can be made for parts of the North Sea for which the amount of experimental data is insufficient.

The nutrient fluxes in box 9 are in the range of observations. It is questionable however whether the highest measured fluxes can be considered as representative for box 9 (Lohse *et al.*, 1993). Neglecting this observation would lead to the conclusion that the mineralization of N and P is too high in the model. Since the deposition of particulate material to the benthos and the total mineralization rates as indicated by the O_2 consumption are in the right order of magnitude, the conclusion must be either that the C/N and C/P ratios in the deposited material are too low or that the nutrients are preferentially buried or removed by the sediment.

In Fig. 22 the relative fluxes at the sediment-water interface, i.e. the fluxes divided by the yearly averaged mineralization are given for box 9 and 11. In general the P-fluxes behave similarly as those of N, however with one important difference in box 9. Here the relative P-flux reaches substantially larger values than the one of N in summer. This is explained by difference in adsorption properties of N and P. Phosphate is modelled as strongly buffered due to adsorption in the oxic and denitrification layer. If the oxygen and nitrate penetration decreases due to enhanced mineralization activity during summer, the adsorption capacity of the sediment decreases resulting in higher pore water

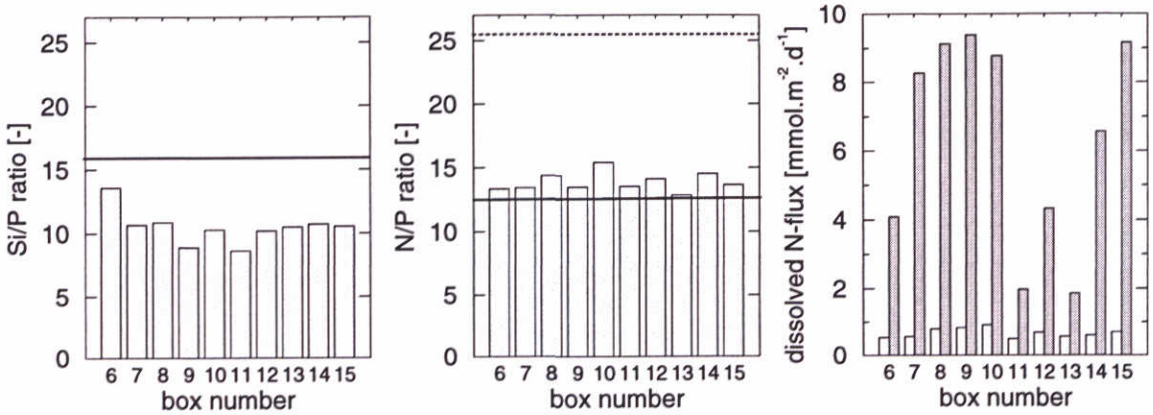

Fig. 24. a. Yearly averaged nutrient ratio of Si/P; b. idem of N/P in the ERSEM-boxes and c. flux of dissolved inorganic N (nitrate + ammonium) in the month February (dark grey) and the month August (light grey). The solid and dotted line in graph a and b stands for the nutrient ratios applied in the model for diatoms and flagellates, respectively.

concentrations and subsequently to higher fluxes at the sediment-water interface. This phenomenon appears not in box 11, here is the concentration of nitrate remains much larger during summer.

The ratios between the nutrient fluxes differ only slightly between the boxes (Fig. 24), however with one dissimilarity for silica. Box 6 shows a distinctly larger Si/P ratio in the fluxes than the other boxes. This is caused by the different morphological properties of this box. In box 6 a deep but fully mixed water column exists and consequently the average light climate is less favourable than in the other boxes. Thus the primary production period is shorter. As a consequence the relative deposition of diatoms is larger than that of flagellates (Varela *et al.*, 1995).

The quality of the results depends on the mutual interference between all the different submodels. The overall picture of the relative importance of the benthic nutrient processes is a result of the dynamics of the whole model: the primary production process, all grazing processes, and all regeneration processes in the benthic and in the pelagic. The percentage of the primary production mineralized in the sediment varies between 20% in off-shore boxes and 60% in coastal boxes (Fig. 23). Compared with estimations by Wollast (1991) (30 to 40%) and by Upton *et al.* (1993) (16 to 55 %) this is at the high side, particularly in the coastal boxes. Apparently, the nutrient input to the benthos as simulated by the model is too high.

Deposition of organic matter is directly coupled to local primary production in ERSEM. Effects of a possible sequence of deposition and erosion events (Jago *et al.*, 1993) by which particulate organic matter is gradually transported from *e.g.* the Southern Bight of the North Sea to the depocentres in the German Bight the and the Skagerrak (Eisma, 1987; Howarth *et al.*, 1993) are not included. Thus, typical differences observed in the field between nutrient dynamics in coarse grained erosion areas and fine grained deposition areas (Van Raaphorst *et al.*, 1992; Lohse *et al.*, 1993; Slomp & van Raaphorst, 1993a) are only partly covered in our model.

Primary production seems adequately modelled in ERSEM. The spring bloom consists largely of diatoms which are assumed to settle on the seafloor when dissolved silica in the water column is depleted without substantial pelagic mineralization (Varela *et al.*, 1995). The resulting mass deposition at the end of the bloom forms the major input of biogenic silica to the seafloor and fur-

ther contains both very labile and more refractory organic matter. The summer deposition mainly originates from flagellates which have gone partly through mineralization processes in the water column. As a result this material is less labile than the spring bloom deposition and contains only small amounts of biogenic silica (Varela *et al.*, 1995; ?). The effect of the spring bloom deposition is clearly recognized in the benthic oxygen consumption rates, the effluxes of ammonium and nitrate, and the nitrification and denitrification rates in the shallow coastal boxes (*e.g.* box 9 in the German Bight). The effect on the phosphate and silica fluxes is less pronounced due to the strong adsorption capacity of the oxic sediments for phosphate that buffers short term phosphate inputs, and because silica dissolution from diatom frustules is a relatively slow process. Thus, the silica effluxes during summer are caused by the dissolution of biogenic silica derived from the diatom deposition in spring.

Differences between the boxes are caused by water transport between the boxes and morphological properties of the boxes as depth and light climate. Joint & Pomroy (1993) report for the ERSEM boxes 8 and 9 larger primary production than for box 7 and 15 (Fig. 8). Our model, however, generates only small differences between these boxes. An unrealistic result of the model is the very high primary production in box 2/12 and 4/14. As a consequence the calculated deposition of organic matter in box 7 and 15 and probably also in box 12 and 14 are too high. Model results on nutrient fluxes from the sediment (Fig. 24c) in these boxes may thus also be too large.

According to our knowledge, there are no reliable data to compare with the deposition of organic matter calculated by the ERSEM model. There are, however, several data sets on oxygen consumption by North Sea sediments. Cramer (1990), Van Raaphorst *et al.* (1992) and Nedwell *et al.* (1993) report oxygen consumptions by southern North Sea sediments between 10 and 75 mmol $O_2 \cdot m^{-2} \cdot d^{-1}$ during summer and less than 20 mmol $O_2 \cdot m^{-2} \cdot d^{-1}$ during winter. Annual carbon oxidation was estimated by these authors at 30 to 100 g $C \cdot m^{-2}$ of which according to Upton *et al.* (1993) 10 to 50% was performed by sulphate reduction. The results generated by our model compare well with these data. We conclude that on average input and mineralization of organic matter in the North Sea sediments are adequately modelled. In the ERSEM model, the North Sea is divided into 10 large boxes. Obviously, in-box details and heterogeneity are lost by this schematisation. In reality, however, substantial differences in sediment composition, organic matter deposition and nutrient early diagenesis can occur within a single box (Rutgers van der Loeff, 1980). Box 9 in the German Bight is a good example for this with coarse sands in the northern half and a deposition area with fine grained sediments in the Helgoland Bight close to the Elbe Mouth (Wiesner *et al.*, 1990). These differences are reflected in the data points included in the Fig. 18 to 21. The model can never reproduce these local variations and this makes detailed comparison with field data a difficult task. Still, the model seems to reasonably simulate box averaged oxygen and nutrient fluxes, at least for box 9 for which detailed data were available.

The modelled profiles of ammonium, nitrate and phosphate reflect non-steady state conditions in the sediments due to the seasonal variations of deposition of organic matter and changing nutrients concentrations in the overlying water. If compared with field observations the nutrient pore water concentrations are fairly well modelled for the first 5 cm of the sediment for box 9 (Figs. 14, 15 and 19). For the lower layers some discrepancies are observed, mainly caused by the absence of slowly degrading organic matter in the model (?).

The phosphate profiles do not reflect the observed low concentrations in the upper few mm's in case of substantial adsorption in the oxic zone of the sediment (Sundby *et al.*, 1992; Slomp & van

Raaphorst, 1993b,Fig. 19). This is probably due to a too simple implementation of the adsorption process. The observed high phosphate concentration in August in box 9 is probably caused by small oxygen and nitrate penetration in the sediment in that period. Because the model does not predict such an anoxic state of the sediment the model results do not reflect these high phosphate porewater concentrations. The simulation of silica profiles is still in a preliminary stage. The dependency of the silica dissolution on both solid biogenic and dissolved silica makes this submodel more complicated than those of the other nutrients. Even with the assumption of exponentially declining biogenic silica contents, the resulting computation scheme is not easily worked out (Appendix 4.3.) and shows that our approximation method (steady states and correction sequence) has its limits. We were, however, able to simulate a clear response of the pore water concentrations to the changing environmental conditions (deposition and temperature) and also obtained reliable Si-effluxes from the sediment.

The general picture that emerges from the model is depletion of organic matter and associated nutrient mineralization in winter and early spring. This conclusion is supported by field data obtained in the Southern Bight (Van Raaphorst *et al.*, 1992). Deposition of fresh organic matter after the spring bloom has dramatic effects on the nutrient processes in the sediment, with increased concentration and fluxes. Similar affects of spring bloom deposition were observed by Jensen *et al.* (1990) in Aarhus Bay. During summer, benthic nutrient cycling is driven by mineralization of organic matter deposited during spring and summer. In agreement with field observations (*e.g.* Van Raaphorst *et al.*, 1992), the model indicates that the largest part of the organic matter is mineralized within a single season. Build up of organic matter of organic matter and nutrients seems to be restricted to the few depostion areas in the North Sea.

Acknowledgements.— This research was partly funded by the European Community under MAST contract number CT90-0021. Additional funds were supplied by BEON (proj. nr. NIOZ 92 E 03). Most field data were obtained from two BELS-cruises financially supported by the Netherlands Marin Research Foundation (grant 39104). We thank Leo Maas for mathematical advice during the devolpment of the model.

REFERENCES

BARETTA, J. W., W. EBENHÖH & P. RUARDIJ, 1995. The European Regional Ecocsystems Model, a complex marine ecosystem model. – Neth. J. Sea Res. **33**, 233–246.

BERNER, R. A., 1976. Inclusion of adsorption in the modelling of early diagenesis. – Earth Planet. Sci. Letters **29**, 333–340.

BERNER, R. A., 1980. Early diagenesis: A theoretical approach. Princeton Univ. Press, Princeton.

BILLEN, G., 1982. An idealized model of nitrogen recycling in marine sediments. – Am. J. Sci. **282**, 512–514.

BOULDIN, D. R., 1968. Models for describing the diffusion of oxygen and other mobile constituents across the mud-water interface. – J. Ecol. **56**, 77–87.

CANFIELD, D. E., B. B. JØRGENSEN, H. FOSSING, R. GLUD, J. GUNDERSEN, N. B. RAMSING, J. W. HANSEN, L. P. NIELSEN & P. O. J. HALL, 1993. Pathways of organic carbon oxidation in three continental margin sediments. – Mar. Geol. **113**, 27–40.

CARSLAW, H. S. & J. C. JAEGER, 1946. Conduction of heat in solids. Oxford University Press, London. 1-510.

CRAMER, A., 1990. Seasonal variation in benthic metabolic activity in a frontal system in the North Sea. In M. Barnes & R. N. Gibson (Eds.), Trophic relationships in the marine environments, pp. 54–76. Aberdeen Univ. Press, Aberdeen.

EBENHÖH, W., C. KOHLMEIER & P. RADFORD, 1995. The benthic biological submodel in the European Regional Seas Ecosystem model. – Neth. J. Sea Res. **3/4**, 423–452.

EISMA, D., 1987. The North Sea: an overview. – Phil. Trans. R. Soc. **316**, 461–485.

FROELICH, P. N., G. P. KLINKHAMMER, M. L. BENDER, N. A. LUEDTKE, G. R. HEATH, D. CULLEN, P. DAUPHIN, D. HAMMOND, B. HARTMAN & V. MAYNARD, 1979. Early oxidation of organic matter in pelagic sediments of the eastern equatorial Atlantic: suboxic diagenesis. – Geochim. cosmochim. Acta **43**, 1075–1090.

GEHLEN, M., 1993. Fluxes of dissolved silica across the sediment-water interface. In W. van Raaphorst & J. P. Boon (Eds.), The Integrated North Sea Programme 1991-1992, preliminary results., Volume 9 of *NIOZ-report*. NIOZ, Texel.

GOLOWAY, F. & M. BENDER, 1982. Diagenetic models of interstitial nitrate profiles in deep sea sediments. – Limnol. Oceanogr. **27**, 624–638.

HENRIKSEN, K. & W. M. KEMP, 1988. Nitrification in estuarine and coastal marine environments. In T. H. Blackburn & J. Sørensen (Eds.), Nitrogen cycling in coastal marine environments, Volume 33 of *SCOPE*, pp. 207–249. Wiley & Sons, New York.

HOWARTH, M. J., K. R. DYER, I. R. JOINT, D. J. HYDES, D. A. PURDIE, H. EDMONDS, J. E. JONES, R. K. LOWRY, T. J. MOFFAT, A. J. POMROY & R. PROCTOR, 1993. Seasonal cycles and their spatial variability. – Phil. Trans. R. Soc. **343**, 383–402.

JAGO, C. F., A. J. BALE, M. O. GREEN, M. J. HOWARTH, S. E. JONES, I. N. MCCAVE, G. E. MILLWARD, A. W. MORRIS, A. A. ROWDEN & J. J. WILLIAMS, 1993. Resuspension processes and seston dynamics, southern North Sea. – Phil. Trans. R. Soc. **343**, 475–488.

JAHNKE, R. A., S. R. EMERSON & J. W. MURRAY, 1982. A model of oxygen reduction, denitrification and organic matter mineralization in marine sediments. – Limnol. Oceanogr. **27**, 610–623.

JENSEN, M. H., E. LOMSTEIN & J. SØRENSEN, 1990. Benthic NH_4^+ and NO_3^- flux following sedimentation of a spring phytoplankton bloom in Aarhus Bight, Denmark. – Mar. Ecol. Prog. Ser. **61**, 87–96.

JOINT, I. & A. POMROY, 1993. Phytoplankton biomass and production in the southern North Sea. – Mar. Ecol. Prog. Ser. **99**, 169–182.

JØRGENSEN, B. B., 1989. Sulphate Reduction in marine sediments from the Baltic Sea-North Sea transition. – Ophelia **31**, 1–15.

KROM, M. D. & R. A. BERNER, 1980. The diagenesis of phosphorus in a nearshore marine sediment. – Geochim. cosmochim. Acta **45**, 207–216.

LOHSE, L., J. F. P. MALSCHAERT, C. P. SLOMP, W. HELDER & W. VAN RAAPHORST, 1993. Nitrogen cycling in North Sea sediments: interaction of denitrification and nitrification in offshore and coastal areas. – Mar. Ecol. Prog. Ser. **101**, 283–296.

MACKIN, J. E. & R. C. ALLER, 1984. Ammonium adsorption in marine sediments. – Limnol. Oceanogr. **29**, 250–257.

NEDWELL, D. B., R. J. PARKER, A. C. UPTON & D. J. ASSINDER, 1993. Seasonal fluxes across the sediment-water interface, and processes within sediments. – Phil. Trans. R. Soc. **343**, 519–531.

PETERSON, B. J., 1980. Aquatic primary productivity and the ^{14}C-CO_2 method: a history of the productivity problem. A. – Rev. Ecol. Syst. **11**, 359–389.

PRESS, W. H., B. P. FLANNERY, S. A. TEUKOLSKY & W. T. VETTERLING, 1986. Numerical recipes. The art of Scientific Computing. Cambridge University Press, Cambridge.

RUARDIJ, P. & W. VAN RAAPHORST, 1995. Benthic nutrient regeneration in the ERSEM ecosystem model of the North Sea. – Neth. J. Sea Res. **3/4**, 453–483.

RUTGERS VAN DER LOEFF, M. M., 1980. Nutrients in the interstitial waters of the Southern Bight of the North Sea. – Neth. J. Sea Res. **14**, 144–171.

SLOMP, C. P. & W. VAN RAAPHORST, 1993a. Forms of phosphorus in North Sea sediments and fluxes across the sediment-water interface. In W. van Raaphorst & J. P. Boon (Eds.), The Integrated North Sea Programme 1991-1992, preliminary results., Volume 9 of *NIOZ-report*, pp. 20–23. NIOZ, Texel.

SLOMP, C. P. & W. VAN RAAPHORST, 1993b. Phosphate adsorption in oxidized marine sediments. – Chem. Geol. **107**, 477–480.

SUNDBY, B., V. GOBEIL, N. SILVERBERG & A. MUCCU, 1992. The phosphorus cycle in coastal marine sediments. – Limnol. Oceanogr. **37**, 1129–1145.

UPTON, A. C., D. B. NEDWELL, R. J. PARKES & S. M. HARVEY, 1993. Seasonal benthic microbial activity in the southern North Sea; oxygen uptake and sulphate reduction. – Mar. Ecol. Prog. Ser. **101**, 273–281.

VAN RAAPHORST, W., H. T. KLOOSTERHUIS, E. M. BERGHUIS, A. J. M. GIELES, J. F. P. MALSCHAERT & G. J. VAN NOORT, 1992. Nitrogen cycling in two types of sediments of the southern North Sea (Frisian Front, Broad Fourteens): field data and mesocosm results. – Neth. J. Sea Res. **28**, 293–316.

VAN RAAPHORST, W., H. T. KLOOSTERHUIS, A. CRAMER & K. J. M. BAKKER, 1990. Nutrient early diagenesis in the sandy sediments of the Dogger Bank area, North Sea: pore water results. – Neth. J. Sea Res. **26**, 25–52.

VAN RAAPHORST, W., P. RUARDIJ & A. G. BRINKMAN, 1988. The assessment of benthic phosphorus regeneration in an estuarine ecosystem model. – Neth. J. Sea Res. **22**, 23–36.

VANDERBORGHT, J.-P. & G. BILLEN, 1975. Vertical distribution of nitrate concentration in interstitial water of marine sediments with nitrification and denitrification. – Limnol. Oceanogr. **20**, 953–961.

VANDERBORGHT, J.-P., R. WOLLAST & G. BILLEN, 1977. Kinetic models of diagenesis in disturbed sediments. Part 2. Nitrogen diagenesis. – Limnol. Oceanogr. **22**, 794–803.

VARELA, R. A., A. CRUZADO & J. E. GABALDÓN, 1995. Modelling Primary production in the North Sea using ERSEM. – Neth. J. Sea Res. **xx**, xxx–xxx.

WIESNER, M. G., B. HAAKE & H. WIRTH, 1990. Organic facies of surface sediments in the North Sea. – Org. Geochem. **15**, 419–432.

WOLLAST, R., 1991. The coastal organic carbon cycle: fluxes, sources and sinks. In R. Mantoura, J.-M. Martin, & R. Wollast (Eds.), Ocean Margin Processes in Global Change, Volume 9 of *physical, chemical, and earth sciences reports*, pp. 365–381. John Wiley & Sons., Chicester.

4. TECHNICAL DESCRIPTION OF GEMDSED

4.1. APPROXIMATION OF THE TRANSIENT PROFILES AND FLUXES

The estimation of the adaptation time t_a is based on the general solution of eq. (2). By substituting $\xi = C - \frac{M}{k}$ eq. (2) becomes:

$$\frac{\partial \xi}{\partial t} = D\frac{\partial^2 \xi}{\partial z^2} - k\xi \tag{10}$$

If the steady-state solution of eq. (10) is taken as the initial condition, say $f(z)$, and if $g(z)$ is the new profile after changing the boundary condition at $t = 0$, the general solution is (Carslaw & Jaeger, 1946):

$$\xi(z,t) = g(t) + \frac{2}{H}\sum_{n=1}^{\infty} b_n e^{-t(k+Dn^2\pi^2)} \sin(n\pi z) \tag{11}$$

in which

$$b_n = \int_{z'=0}^{H} [f(z') - g(z')] \sin(n\pi z')dz' \tag{12}$$

The second term in eq. (11) fully describes the transient state of ξ and thus of C. The dynamics are determined by the exponential terms.

The adaptation time is defined from eq. (11). Taking as criterion the first term in the series and thus neglecting the higher order terms of eq. (11) the adaptation time is approximated by:

$$t_a = \frac{p+1}{k + \pi^2 DH^{-2}} \tag{13}$$

This adaptation time is applied in the following way:

$$F(t + \Delta t) = G(z) + [F(z) - G(z)]e^{-\frac{\Delta t}{t_a}} \tag{14}$$

in which $F(z, t + \Delta t)$ is the concentration present at $t + \Delta t$ at depth z, $F(z)$ is the concentration at depth z the concentration present at t and $G(z)$ the concentration to be obtained for large values of Δ t.

However, in the model we are not interested in concentrations at a time $t + \Delta t$ but in the 'average' profile during a time step. Thus, the average concentration during the time interval $[t, t + \Delta t]$ is calculated as:

$$\overline{F(t \Rightarrow t + \Delta t)} = G(t) + [F(z) - G(z)]\frac{t_a}{\Delta t}(1 - e^{-\frac{\Delta t}{t_a}}) \tag{15}$$

In which the bar over F denotes the time-step averaged profile. From this profile all fluxes and depth-integrated concentrations are calculated.

4.2. DYNAMICAL SOLUTIONS

In section 1.4., two exact dynamical solutions of partial differential equations (PDE's) are applied to compare with the appoximate solutions of the model (Carslaw & Jaeger, 1946). In both cases the solutions are valid of eq. (2) in which $p = 0$:

$$\frac{\partial C}{\partial t} = D\frac{\partial^2 C}{\partial z^2} - kC + M \tag{16}$$

4.2.1. PDE WITH ZERO-ORDER INPUT AND FIRST ORDER LOSS TERM

By substituting $\xi = C - \frac{M}{k}$ eq. (16) becomes:

$$\frac{\partial \xi}{\partial t} = D\frac{\partial^2 \xi}{\partial z^2} - k\xi \tag{17}$$

if the following conditions are fulfilled:

- Mineralization takes place in a finite layer $0 < z < H$.
- Initial constant gradient: ξ_{in} $(0 < z < H)$
- Ends at concentration ξ_0 and ξ_H, respectively at $z = 0$ and $z = H$.

the dynamical solution of eq. (17) is:

$$\xi(z,t) = \frac{2}{H}\sum_{n=1}^{\infty} e^{-t(Dn^2\pi^2H^{-2}+k)}\sin(n\pi z)$$
$$\left\{\xi_{in}(1-\cos(n\pi H))\frac{n\pi D}{H} + \int_{\lambda=0}^{t} e^{\lambda(Dn^2\pi^2H^{-2}+k)}(\xi_0 - (-1)^n\xi_H)\,d\lambda\right\} \tag{18}$$

4.2.2. PDE WITH ZERO-ORDER INPUT

If the following conditions are fulfilled:

- Mineralization takes place in a finite layer $0 < z < H$.
- The surface concentration $C(0) = 0$ for $t \geq 0$
- Initial constant gradient: C_{in} $(0 < z < \infty)$

the dynamical solution of eq. (16) with $k = 0$ becomes:

$$C(z,t) = C_{in}\,\mathrm{erf}\frac{z}{2\sqrt{Dt}} + +Mt\left\{1 - 4\,\mathrm{i}^2\mathrm{erfc}\frac{z}{2\sqrt{Dt}} + 2\,\mathrm{i}^2\mathrm{erfc}\frac{H+z}{2\sqrt{Dt}} - 2\,\mathrm{i}^2\mathrm{erfc}\frac{H-z}{2\sqrt{Dt}}\right\} \tag{19}$$

4.3. GENERAL STEADY-STATE SOLUTIONS

The solutions of the steady-state equations of the partial differential equations (PDE's) are given only in general terms without explicit formulations of the integration constants. The latter are calculated in the model by a Gauss-elimination method.

4.3.1. AMMONIUM

The steady-state solutions for the set of PDE's listed in box 1 for ammonium are:

$$A_1(z) = a_{11}e^{-\gamma z} + a_{12}e^{\gamma z} + a_{15}$$
$$A_2(z) = a_{21}e^{-\alpha\zeta} + a_{24}z + a_{25}$$

in which $a_{11}, a_{12}, a_{24}, a_{25}$ are integration constants, and

$$a_{15} = \frac{M_A}{k}$$
$$a_{21} = \frac{M_A}{D_A\alpha^2}$$
$$\gamma = \sqrt{\frac{k}{D_A}}$$

4.3.2. NITRATE

The steady-state solutions for the set of PDE's listed in box 1 for nitrate are:

$$N_1(z) = n_{11}e^{-\gamma z} + n_{12}e^{\gamma z} + n_{13}z^2 + n_{14}z + n_{15}$$
$$N_2(z) = n_{21}e^{-\beta z}$$

in which n_{14} and n_{21} are integration constants and

$$n_{11} = \frac{a_{11}}{D_N\gamma^2}$$
$$n_{12} = \frac{a_{12}}{D\gamma^2}$$
$$n_{13} = \frac{a_{15}}{2D}$$
$$n_{15} = N_0 - n_{11} - n_{12}$$
$$\beta = \sqrt{\frac{d}{D_N}}$$

γ, a_{11}, a_{12} and a_{15} are listed in the ammonium model. See C.1

4.3.3. PHOSPHATE

The steady-state solutions for the set of PDE's listed in box 2 are:

$$P_1(z) = p_{13}z^2 + p_{14}z + p_{15}$$
$$P_2(z) = p_{21}e^{-\alpha\zeta} + p_{24}z + p_{25}$$
$$P_3(z) = p_{31}e^{-\alpha\zeta} + p_{35}$$

in which p_{14}, p_{24}, p_{25} and p_{35} are integration constants, and

$$p_{13} = P_0$$
$$p_{13} = \frac{M_P}{2D_P}$$
$$p_{21} = \frac{M_P}{D_P\alpha^2}$$
$$p_{31} = \frac{M_P}{e}^{-\alpha(z_{an}-z_{oz})} D_P\alpha^2$$

4.3.4. SILICA

The steady-state solutions for the set of PDE's listed in box **??** are :

$$C_1(z) = c_{13}z^2 + c_{14}z + c_{15}$$
$$C_2(z) = c_{21}I_0(\lambda e^{-\frac{1}{2}\beta\zeta})$$

in which c_{13}, c_{14} and c_{21} are integration constants and

$$c_{15} = \frac{sB_1}{2D_{Si}}$$
$$\lambda = \frac{2}{\beta}\frac{sB_1}{Si_\infty D_{Si}}$$

I_0 stands for the modified Bessel function of 0th order.

4.3.5. REDUCTION EQUIVALENTS

The steady-state solutions for the set of PDE's listed in box 3 are:

$$R_1(z) = r_{13}z^2$$
$$R_2(z) = r_{21}e^{-\alpha\zeta} + r_{22}e^{-\beta z} + r_{25}$$

in which r_{25} is an integration constant and

$$r_{13} = \frac{M_r}{2D_R}$$
$$r_{21} = \frac{M_O}{\eta_r D_R \alpha^2}$$
$$r_{22} = -\frac{dn_{21}}{D_R\beta^2}$$

The definitions of β, n_{21} are given in the nitrate model (C.2).

4.3.6. OXYGEN

The steady-state solution for the differential equation listed in box 4 is:

$$Ox(z) = o_{13}z^2 + o_{14}z + n_{15}$$

in which o_{13} and o_{14} are integration constants and

$$o_{15} = Ox_0$$

4.4. THE NUTRIENT MODELS

4.4.1. INTRODUCTION

This model calculates fluxes from which step the new values of the state variabels are derived. For the calculation of the fluxes of ammonium, nitrate, reduction equivalent and silicate the same basic scheme is used. Each of the following chapters starts with a mathematical description of the set of differential equations which is applied. It consists of the description of the set of differential equations itself and the set of solution equations. Thereafter the input to the submodel is described. The central part of each chapter consists of a description of the calculations to derive the fluxes:

1. Calculate the actual values of the parameters of the submodel: correct for the environmental conditions
2. Define a set of solution equations for the set of differential equations and the related boundary and continuity conditions and calculate the equilibrium profile on the basis of the actual parameter values.
3. Calculate from this profile the average concentration G(t) in the layer for which the state variable is defined (=F(t))
4. Calculate the adaptation time t_a
5. Calculate an average concentration $\overline{F(t \Rightarrow t + \Delta t)}$ which is an intermediate concentration between G(t) and F(t) and is the expected concentration during the following time step.
6. Define the set of solution equations of the set of differential equations plus the related boundary and continuity conditions and calculate the steady-state profile on the basis of this intermediate state.
7. Calculate the fluxes from the steady-state profile.

4.4.2. MATHEMATICAL DESCRIPTION OF THE AMMONIUM MODEL

Parameters:

k: specific nitrification rate (day^{-1})

xdiffK4 ($= D_a$): whole sediment diffusion constant (m^{-2} day^{-1}).

α: constant, describing the exponential decrease of mineralization with depth (m^{-1}).

p_a: adsorption distribution coefficient of ammonium. (-)

Forcing

- Forcing functions:

  ETW: temperature of the water column(°C). It is assumed that the temperature in the sediment is equal to the the water temperature.

  irrenh: bioirrigation constant. (-) Multiplication factor describing the enlargement of the molecular diffusion caused by activity of benthic organisms.

- Rates:

  reBTn: oxic ammonium mineralization (mmol N m^{-2} day^{-1}); this rate is obtained from the GEM model.

  reATn: anoxic ammonium mineralization (mmol N m^{-2} day^{-1}); this rate is obtained from the GEM model.

- State variables:

  K4n: ammonium concentration integrated over the depth of the upper layer (mmol N m^{-2})

  K14n: idem, integrated over the denitrification + anoxic layer. (mmol N m^{-2})

  N4n: ammonium concentration in the watercolumn above the sediment. (mmol N m^{-3})

Output fluxes: All fluxes of ammonium are estimated from the profile $A_{tr}(z)$: For the calculation of the transient profile see Section 1.4..

- flux across the sediment-water interface (mmol N m^{-2} day^{-1}):

$$jK4N4n = \phi D_a \frac{\partial A_{tr}(0)}{\partial z}$$

- nitrification (mmol N m^{-2} day^{-1}):

$$jK4K3n = \phi k(p_a + 1)\phi \int_{z=0}^{D1m} A_{tr}(z)dz$$

- flux from NH4S2 to NH4S1 (mmol N m^{-2} day^{-1}):

$$jK14K4n = \phi D_a \frac{\partial A_{tr}(D1m)}{\partial z}$$

- flux from the sediment below the depth of 30 cm to NH4S2 (source) (mmol N m^{-2} day^{-1}):

$$jK24K14n = \phi D_a \frac{\partial A_{tr}(Dtm)}{\partial z}$$

4.4.3. MATHEMATICAL DESCRIPTION OF THE NITRATE MODEL

Parameters:

k: specific nitrification rate (day^{-1})

d: specific denitrification rate (day^{-1})

xdiffK3 ($= D_n$): whole sediment diffusion constant of nitrate (m^{-2} day^{-1})

Forcing The profiles are further defined and calculated from the following GEM variables:

- Forcing functions:

  ETW: temperature of the water column(°C). It is assumed that the temperature in the sediment is equal to the the water temperature.

  irrenh: bioirrigation constant. (-) Multiplication factor describing the enlargement of the molecular diffusion caused by activity of benthic organisms.

- Profile:

  $A_{tr}(z)$: the ammonium profile: See the ammonium model for the description.

- State variables:

  K3n: nitrate concentration integrated over the depth of the oxic and denitrification layer (mmol N m^{-2})

  N3n: nitrate concentration in the watercolumn above the sediment. (mmol N m^{-3}).

Output fluxe: All fluxes of nitrate are estimated from the profile $N_{tr}(z)$:

- flux across the sediment-water interface (mmol N m^{-2} day^{-1}):

$$jK3N3n = D_n \frac{\partial N_{tr}(0)}{\partial z} \phi$$

- denitrification (mmol N m^{-2} day^{-1}):

$$jK3G4n = d\phi \int_{z=D1m}^{D2m} N_{tr}(z)dz$$

- flux of K3n at D2m (mmol N m^{-2} day^{-1}):

$$jK13K3n = D_n \frac{\partial N_{tr}(D2m)}{\partial z} \phi$$

4.4.4. CALCULATION OF THE DENITRIFICATION DEPTH

The depth of D2m is calculated from the following variables:

Parameters

pmK3n_p: proportion (-).
From this proportion and the concentration of nitrate at D1m the concentration at D2m$_{eq}$ is calculated.
value: 0.10

clM3n_D2m_p: minimum concentration of nitrate at D2m (mmol N m^{-3})
value: 0.5

clD12m_p: minimum thickness of the denitrification layer (m).
value:0.01

Profile:

N_{tr}(z): nitrate profile : See the nitrate model for the description.

Other variables:

β: variable which describes the exponential decrease of nitrate (m^{-1}). This calculated from

$$\beta = \sqrt{\frac{d}{D_n}} \tag{20}$$

in which d and D_n are the denitrification rate and the diffusion constant of nitrate. See further nitrate model.

Acutal Calculation The thickness D2m is derived in the following way:

1. Calculation of the nitrate concentration at depth D2m:

$$N_{tr}(D2m) = \max(pmK3n\_p \cdot N_{tr}(D1m), clM3n\_D2m\_p)$$

At a very low nitrate concentration this variable is equal to the parameter $clM3n\_D2m\_p$

2. Calculation of the proportion between the concentration at D2m and the concentration at D1m:

$$pmK3n = \frac{N_{tr}(D2m_{eq})}{N_{tr}(D1m)}$$

3. Calculation of the new depth:

$$D2m = \max(clD12m\_p, \frac{\log(pmK3n)}{\beta}) + D1m$$

4.4.5. Mathematical Description of the Phosphate Model

Parameters:

xdiffK1 ($= D_p$): whole sediment diffusion constant ($m^{-2}day^{-1}$).

α: constant, describing the exponential decrease of mineralization with depth (m^{-1}).

$p_{p,ox}$: adsorption distribution coefficient of phosphate in the oxic and denitrification layer. (-).

$p_{p,an}$: adsorption distribution coefficient of phosphate in the anoxic layer. (-).

Forcing:

- Forcing functions:

ETW: temperature of the water column(°C). It is assumed that the temperature in the sediment is equal to the the water temperature.

irrenh: bioirrigation constant. (-) Multiplication factor describing the enlargement of the molecular diffusion caused by activity of benthic organisms.

- Rates:

reBTp: the oxic mineralization (mmol P m^{-2}); this rate is obtained from the benthic carbon cycle model.

reATp: the anoxic mineralization (mmol P.m^{-2}); this rate is obtained from the benthic carbon cycle model.

- State variables:

K1p: phosphate concentration integrated over the depth of the oxic (mmol P m^{-2}).

K11p: phosphate concentration integrated over the depth of the anoxic layer (mmol P m^{-2}).

N1p: concentration of phosphate in the water (mmol P m^{-3}).

Output fluxes: All phosphate fluxes are calculated from the transient profile $P_{tr}(z)$:

- flux across the sediment-water interface (mmol P $m^{-2}day^{-1}$):

$$jK1N1p = \phi D_p \frac{\partial P_{tr}(0)}{\partial z}$$

- flux from K11p to K1p (mmol P $m^{-2}day^{-1}$):

$$jK11K1p = \phi D_p \frac{\partial P_{tr}(D2m)}{\partial z}$$

- flux from the sediment below the depth of 30 cm to K11p. (source). (mmol P $m^{-2}day^{-1}$):

$$jK11K1p = \phi D_p \frac{\partial P_{tr}(Dtm)}{\partial z}$$

4.4.6. Mathematical Description of the Reduction Equivalent Model

Parameters

d: specific denitrification rate (mmol O_2· mmol N^{-1} day^{-1})

xdiffK6 ($= D_r$): diffusion constant(m^{-2} day^{-1})

α: constant, describing the exponential decrease of mineralization with depth (m^{-1})

Forcing to the model The profiles are further specified and calculated from the following GEM variables:

- Forcing functions:

ETW: temperature of the water column(°C). It is assumed that the temperature in the sediment is equal to the the water temperature.

irrenh: bioirrigation constant. (-) Multiplication factor describing the enlargement of the molecular diffusion caused by activity of benthic organisms.

- Profile:

$N_{tr}(z)$: the nitrate profile: See the nitrate model for the description.

- Rates:

rrBTo: oxic mineralization rate (mmol O_2 m^{-2} day^{-1}); this rate is obtained from the benthic carbon cycle model.

rrATo: the anoxic mineralization rate (mmol O_2 m^{-2} day^{-1}); this rate is obtained from the benthic carbon cycle model.

- State variables:

K6e: reduction equivalents concentration integrated over the depth of 30 cm (mmol $O_2.m^{-2}$)

enditemize

Output fluxes All fluxes of reduction eqauivalents are calculated from the transient profile $R_{tr}(z)$:

- oxidation of reduction equivalents (mmol $O_2 m^{-2}$ day^{-1}):

$$jK6K7e = sOS \int_{z=0}^{D1m} R_{tr}(z) \cdot \phi$$

- denitrification (mmol N m^{-2} day^{-1}):

$$jK4G4e = d \cdot \phi \cdot \int_{z=D1m}^{D2m} N_{tr}(z)dz$$

- flux from the under layer to K6e (mmol $O_2 m^{-2}$ day^{-1}):

$$jK16K6e = D_r \frac{\partial R_{eq}(D2m)}{\partial z} \phi$$

4.4.7. Mathematical Description of the Oxygen Model

Parameters

D_o: diffusion constant ($m^{-2} day^{-1}$)

$qoK4n\_p$: diffusion constant ($m^{-2} day^{-1}$)

Forcing

Forcing functions:

ETW: temperature of the water column(^oC). It is assumed that the temperature in the sediment is equal to the the water temperature.

irrenh: bioirrigation constant. (-) Multiplication factor describing the enlargement of the molecular diffusion caused by activity of benthic organisms.

- Rates;

rrBTo: the oxic mineralization (mmol O_2 m^{-2} day^{-1})

jK4K3n: nitirifcation (mmol N m^{-2} day^{-1});
Calculated in the Ammonium model.

jK6K7e: oxidation of reduction equivalents in the oxic layer.
(mmol $O_2 m^{-2}$ day^{-1});
Calculated in the Reduction equivalent model.

- State variables:

G2o : oxygen concentration in the oxic layer (mmol O_2 m^{-2})

D1m: thickness of the oxic layer (m).

- Other variables:

O2o: : oxygen in the water column (mmol O_2 m^{-3}) [pelagic state variable:]

Output fluxes:

- flux from the sediment to the water column (mmol O_2 $m^{-2}day^{-1}$) :

$$jG2O2o = G2o - G2oeq - jK6K7e - qoK4n_{p\_}p \cdot jK4K3n - rrBTo$$

CONTENTS

List of Figures

List of Tables

WL | Delft Hydraulics

Rotterdamseweg 185
postbus 177
2600 MH Delft
telefoon 015 285 85 85
telefax 015 285 85 82
e-mail info@wldelft.nl
internet www.wldelft.nl

Rotterdamseweg 185
p.o. box 177
2600 MH Delft
The Netherlands
telephone +31 15 285 85 85
telefax +31 15 285 85 82
e-mail info@wldelft.nl
internet www.wldelft.nl